No. 4 1971

Technical Review

To Advance Techniques in Acoustical, Electrical and Mechanical Measurement

Elastic Modulus
Equivalent Circuit Diagrams
Estimation of Sound Pressure Levels

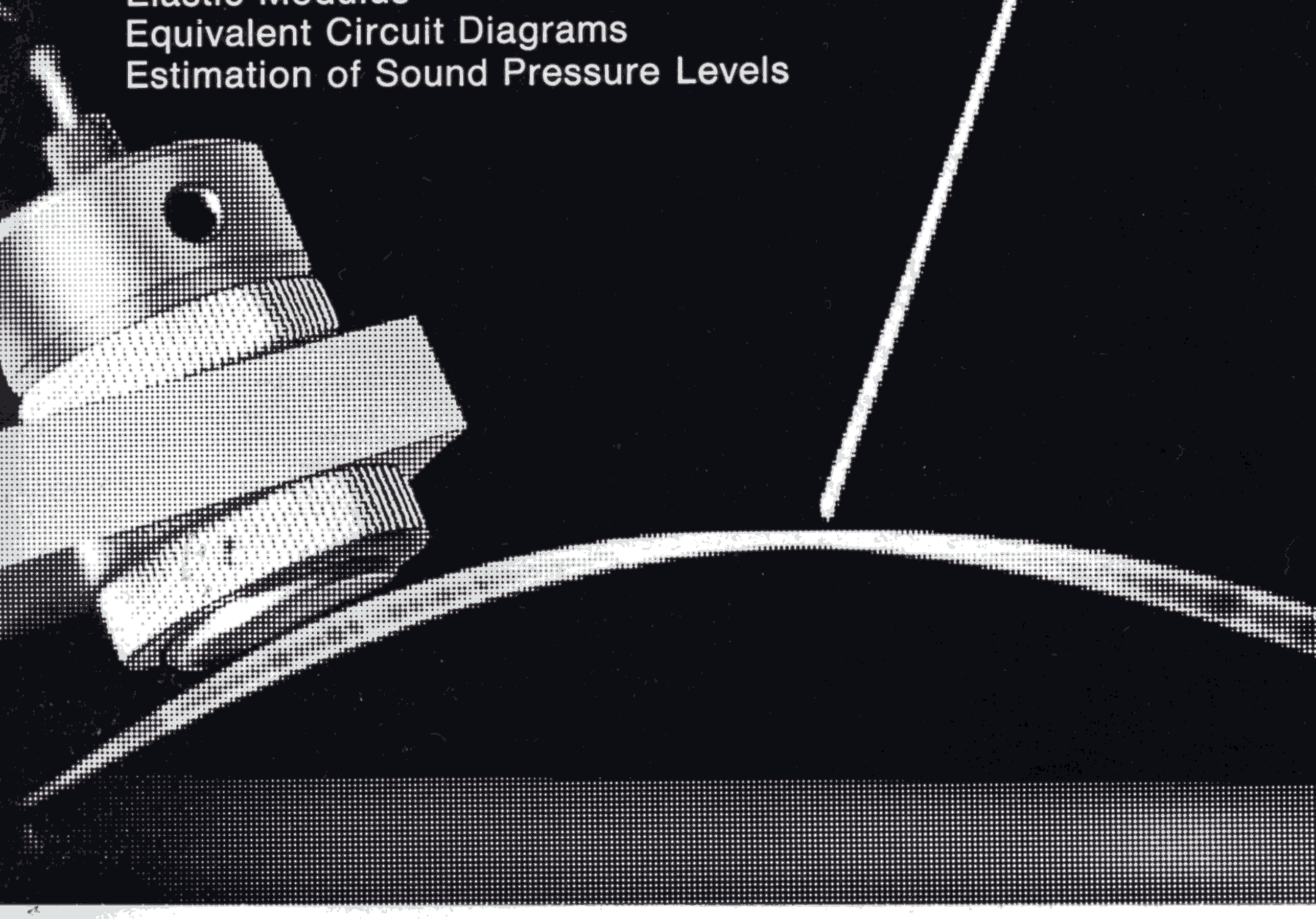

BRÜEL & KJÆR

PREVIOUSLY ISSUED NUMBERS OF BRÜEL & KJÆR TECHNICAL REVIEW

3–1971 Conventional & On-line Methods of Sound Power Measurements.
An Experimental Channel Selector System.

2–1971 Interchangeable Head Vibration Exiters.
AEROS: A Generalized-Spectrum Vibration-Control System.

1–1971 Shock and Vibration Isolation of a Punch Press.
Vibration Measurement by a Laser Interferometer.
A portable Calibrator for Accelerometers.
Electro Acoustic Ear Impedance Indicator for Medical Diagnosis.

4–1970 On the Applicability and Limitations of the Cross-Correlation and Cross-Spectral Density Techniques.

3–1970 On the Frequency Analysis of Mechanical Shocks and Single Impulses.
Important Changes to the Telephone Transmission Measuring System.

2–1970 Measurement of the Complex Modulus of Elasticity of Fibres and Folios.
Automatic Recording-Control System.

1–1970 Acoustic Data Collection and Evaluation with the Aid of a Small Computer.
1/3 Octave Spectrum Readout of Impulse Measurements.

4–1969 Real Time Analysis.
Field Calibration of Accelerometers.
The Synchronization of a B & K Level Recorder Type 2305 for Spatial Plotting.

3–1969 Frequency Analysis of Single Pulses.

2–1969 The Free Field and Pressure Calibration of Condenser Microphones using Electrostatic Actuator.
Long Term Stability of Condenser Microphones.
The Free Field Calibration of a Sound Level Meter.
Accelerometer Configurations.
Vibration Monitoring and Warning Systems.

1–1969 The Use of Digital Systems in Acoustical Measurements.
Impulse Noise Measurements.
Low Frequency Measurements Using Capacitive Transducers.
Details in the Construction of a Piezo-electric Microphone.
A New Method in Stroboscopy.

4–1968 On the Damaging Effects of Vibration.
Cross Spectral Density Measurements with Brüel & Kjær Instruments. (Part II).

(Continued on cover page 3)

TECHNICAL REVIEW

No. 4 – 1971

Contents

Application of Electro-Acoustical Techniques to the Determination of the Modulus of Elasticity by a Non-Destructive Process

by

D. Blay, L. Bourgain and G. Samson *)

ABSTRACT

Electroacoustical, and in general all contact-less measurement techniques which do not disturb the physical phenomena to be measured are very useful to measure the critical frequencies, in flexure, torsion or compression, of shafts on elastic bearings. Thus, combined with digital computer calculations, such methods facilitate the determination of the modulus of elasticity for isotropic, orthotropic and composite materials. The methods have furthermore proven to be very convenient for detection of cracks and flaws in test samples or production specimens.

This paper shows, especially, that dynamic analysis with flexural waves, a method which was abandoned for many years, now again has validity as a simple, rapid and very accurate method to determine the modulus of elasticity of non-standardized beams or test models in a non-destructive way.

Thus, the variations of the modulus of elasticity due to chemical, thermal or other physical treatments as, for example, cold deformation, can be easily evaluated.

SOMMAIRE

Lorsque l'on veut mesurer avec précision les fréquences critiques de flexion, de torsion ou de compression d'un milieu déformable, tel un arbre de machine tournante, il est souhaitable de ne pas perturber le phénomène observé. A cet égard, les techniques acoustiques et plus généralement les techniques de mesure sans contact, sont très appropriées. Lorsque ces dernières sont exploitées sur le plan théorique par un ordinateur, elles permettent de déterminer les modules d'élasticité de matériaux isotropes, orthotropes et composites. Ces méthodes sont aussi très adaptées à la détection des criques et défauts de pièces élaborées en chaine de production.

Dans sa plus grande partie, ce papier montre que la méthode dynamique par ondes de flexion, qui a été abandonnée depuis plusieurs années, s'avère cependant être une méthode simple, rapide, précise et non destructive pour déterminer les modules d'élasticité d'échantillons non standardisés. Elle permet aussi d'apprécier les variations des caractéristiques élastiques du milieu quand celui-ci a été soumis à des traitements chimiques, thermiques ou physiques tels que le fluotournage.

---

*) Centre d'Etudes Nucleaires, 91 Saclay, France. Departement Physico-Chimie.

ZUSAMMENFASSUNG

Berührungslose elektroakustische Meßmethoden, welche die zu messenden physikalischen Vorgänge nicht stören, sind sehr nützlich zur Messung der kritischen Frequenzen bei Biege-, Torsions- oder Längsschwingungen elastisch gelagerter Wellen. Mit Hilfe von Computern ermöglichen solche Methoden die Bestimmung des Elastizitätsmoduls isotroper, orthotroper und zusammengesetzter Werkstoffe. Darüber hinaus haben sich diese Methoden als sehr zweckmäßig erwiesen, um Sprünge und Risse in Materialproben oder Werkstücken zu erkennen.

Insbesondere wird gezeigt, daß die dynamische Analyse mit Biegewellen — eine Methode, die man jahrelang vernachlässigt hatte — heute wieder ihre Berechtigung besitzt als eine einfache, schnelle und sehr genaue Methode zur Bestimmung des Elastizitätsmoduls nicht standardisierter Stäbe oder Prüfkörper. Auf diese Weise lassen sich Änderungen des dynamischen Elastizitätsmoduls infolge chemischer, thermischer oder physikalischer Materialbehandlung, z.B. Kaltverformung, einfach ermitteln.

Introduction

Nowadays engineers responsible for the design and manufacture of rotating machines tend to design rotating parts of ever-increasing angular velocity. However, the methods generally used, such as Stodola's method or that of concentrated masses, prove inaccurate as the order of critical velocity increases. For this reason it was decided to solve the partial differential equations which govern the movements of such structures. Thereby exact solutions and, hence, excellent agreement between theory and experiment (within 0.5%) were obtained.

However, considerable differences between theory and experiments have recently been recorded on hollow, flow turned shafts, a fact which could only be explained by suspecting the value adopted for Young's modulus. Flow turning, like other cold deformation methods, modifies the crystal orientation of the material considerably and produces high level internal stresses. The theory was then put forward that the method not only affected the mechanical, tensile and elongation properties (which is well known), but also the modulus of elasticity.

A search for simple and accurate methods to measure these moduli in order to test the theory led to the dynamic method using flexural waves with the sample resting on two flexible supports. It will be demonstrated that in most cases the frequencies measured correspond to those of a free-free beam and that the modulus values deduced from them are extremely precise provided the shearing stresses and the rotation of the sections are included in the analysis. In this way it was possible to determine the influence of cold deformation processes on the elastic modulus value of the materials.

Methods of Elastic Modulus Measurements

The methods of measuring the moduli of elasticity can be divided into two main categories, static and dynamic.

Static methods are all based on the measurement of the load and the corresponding strain, the tensile test specimen being the simplest example. With modern universal testing machines the curve $F/(\Delta l/l)$ (stress over strain) can be plotted directly and accurately as shown in Fig.1. The modulus is simply determined from the ratio of the two quantities measured. In reality the evaluation is more complicated, as the quantity $F/(\Delta l/l)$ and, hence, the modulus varies with the load. The modulus E_s which is determined by this method is smaller than the modulus E_t at the origin. In vibration mechanics when generally only small movements around an equilibrium position are considered the latter modulus is chiefly involved and therefore called a dynamic modulus.

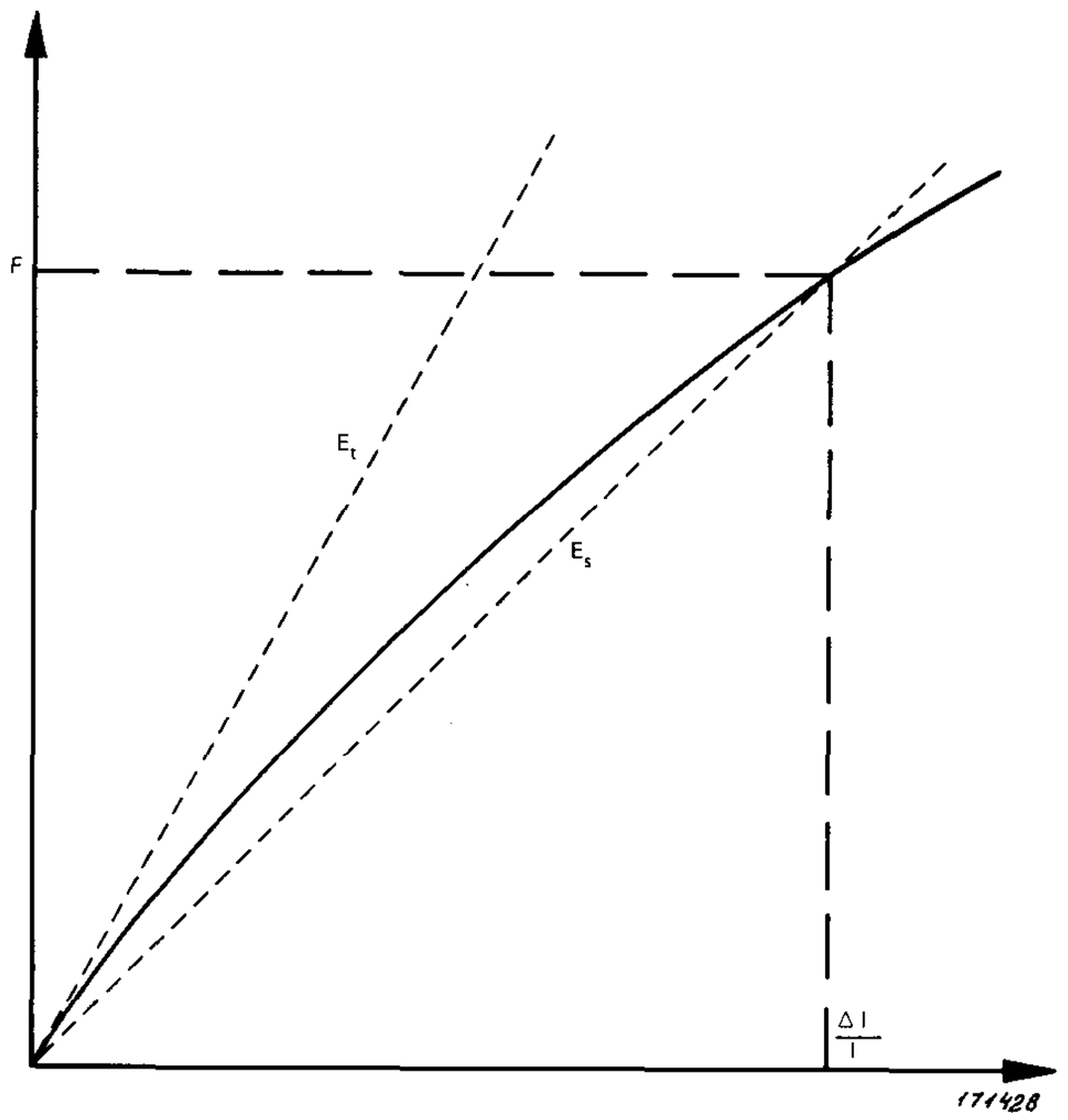

Fig.1. Static Stress-strain curve

In addition, the longitudinal deformation in the tensile test is accompanied by a decrease in cross-section for which the directly obtained curve must be corrected. In some cases the deformation curve also depends on the rate of application of the load and, finally, it is not always possible to take standardized specimens from materials selected for modulus measurements — either because of the size of the available samples, or because non-destructive measurements are required.

Generally, all static methods present the same type of difficulty as that arising by elongation of a rod subjected to a uniaxial stress. Static methods were therefore rejected in favour of dynamic methods of which the method of compression waves is most commonly used.

However, when a somewhat complex structure is excited by trains of compression waves it is found that the longitudinal motions are disturbed by other vibration modes. Consequently it becomes very difficult to identify the different resonances recorded. This has been confirmed in the case of thin-walled cylinders. On the other hand, when the structure is excited transversely identification presents no problem since the positions of the vibration nodes and antinodes are easily determined. Their number indicates the order of the excited mode.

This fact led to an attempt to uncover why flexural methods had been abandoned although they were developed earlier than compression methods. The reason seemed to be the difficulty of analysis and, in fact, it must be acknowledged that the necessary allowances for effects due to shearing stresses and cross-section rotations complicate the analysis. Hence, it is almost impossible to calculate the natural frequencies of the structure without the aid of a computer. To reduce computer time to a minimum, nomographs and tables of figures were established.

The flexural wave method would also have been rejected if it had been necessary, as usually recommended, to hang the test specimen by strings at given points. However, as it could be proven that a sample resting on elastic supports of low rigidity can be considered free in space, for certain conditions, the method was further developed to measure flexural waves without contact.

Theoretical Aspects

In the appendix is given the general theory for bending of constant cross-section beams. From this, the equations of motion are developed for two special cases; first, a beam resting on two elastic supports, where the effects of shear forces and cross-section rotations are neglected and second, a beam free in space with consideration of both shear forces and cross-section rotations.

As shown in the appendix the simplified equation of motion for a beam is

$$\rho S \frac{\partial^2 U}{\partial t^2} + EI \frac{\partial^4 U}{\partial x^4} = O \qquad (1)$$

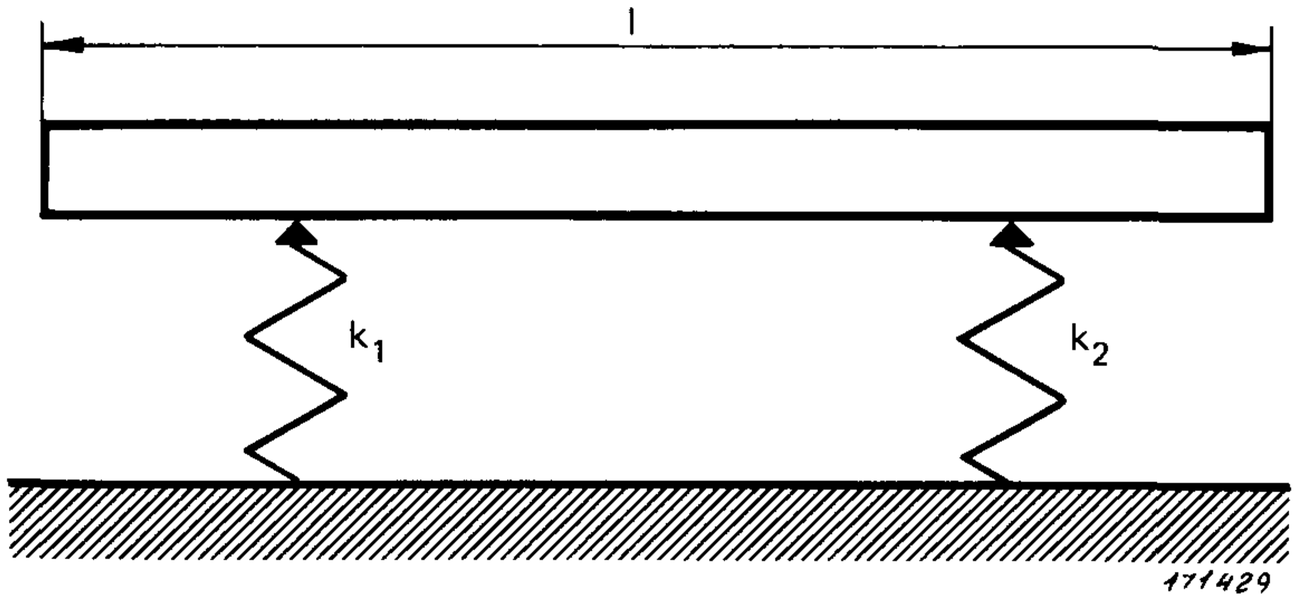

Fig.2. A beam resting on two elastic supports

For a beam resting on two elastic supports (Fig.2) the solutions of the equation have the form

(2)

$$U(x,t) = (A \cos mx + B \sin mx + C \cosh mx + D \sinh mx) \cos(\omega t + \psi)$$

For the given end conditions, the natural frequencies are

$$N_i = \frac{X_i^2}{2\pi}\sqrt{\frac{EI}{\rho S l^4}} \qquad (3)$$

where X_i is a dimensionless constant dependent on the order of the natural mode and on the value of the support stiffnesses k_1 and k_2.

The natural frequencies N_i and the factors X_i have been calculated for beams supported at their extreme ends with equal support stiffness $k = k_1 = k_2$ as shown in Fig.3.

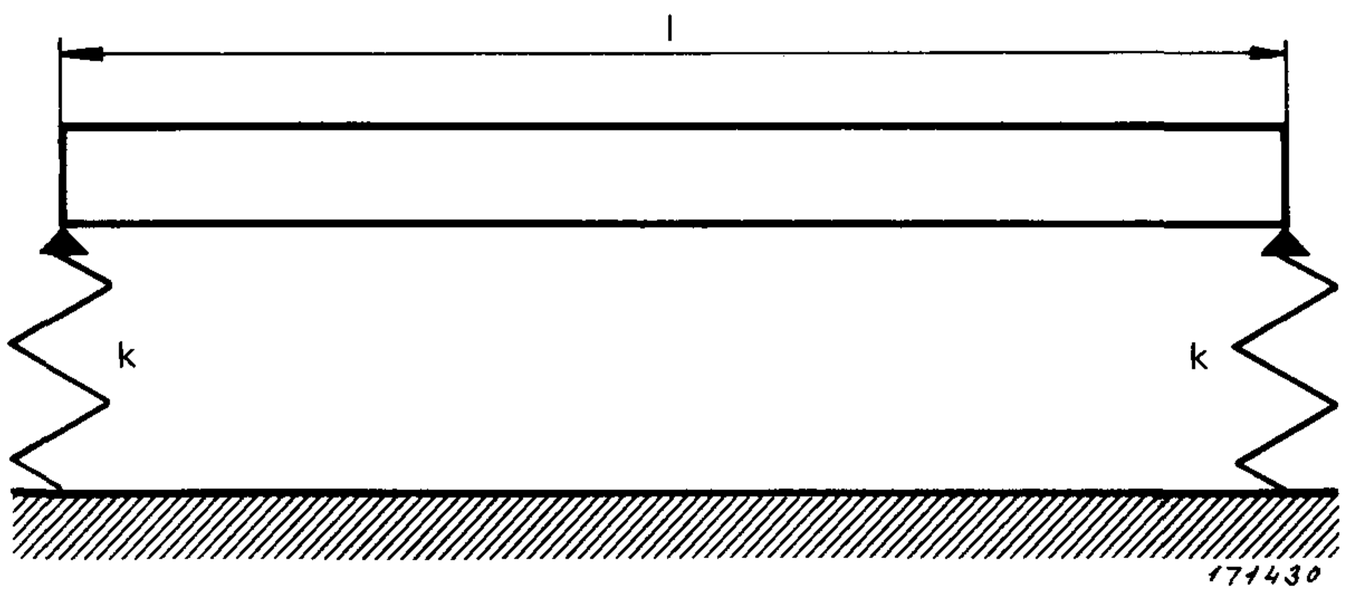

Fig.3. A beam resting on two elastic supports placed at its extreme ends

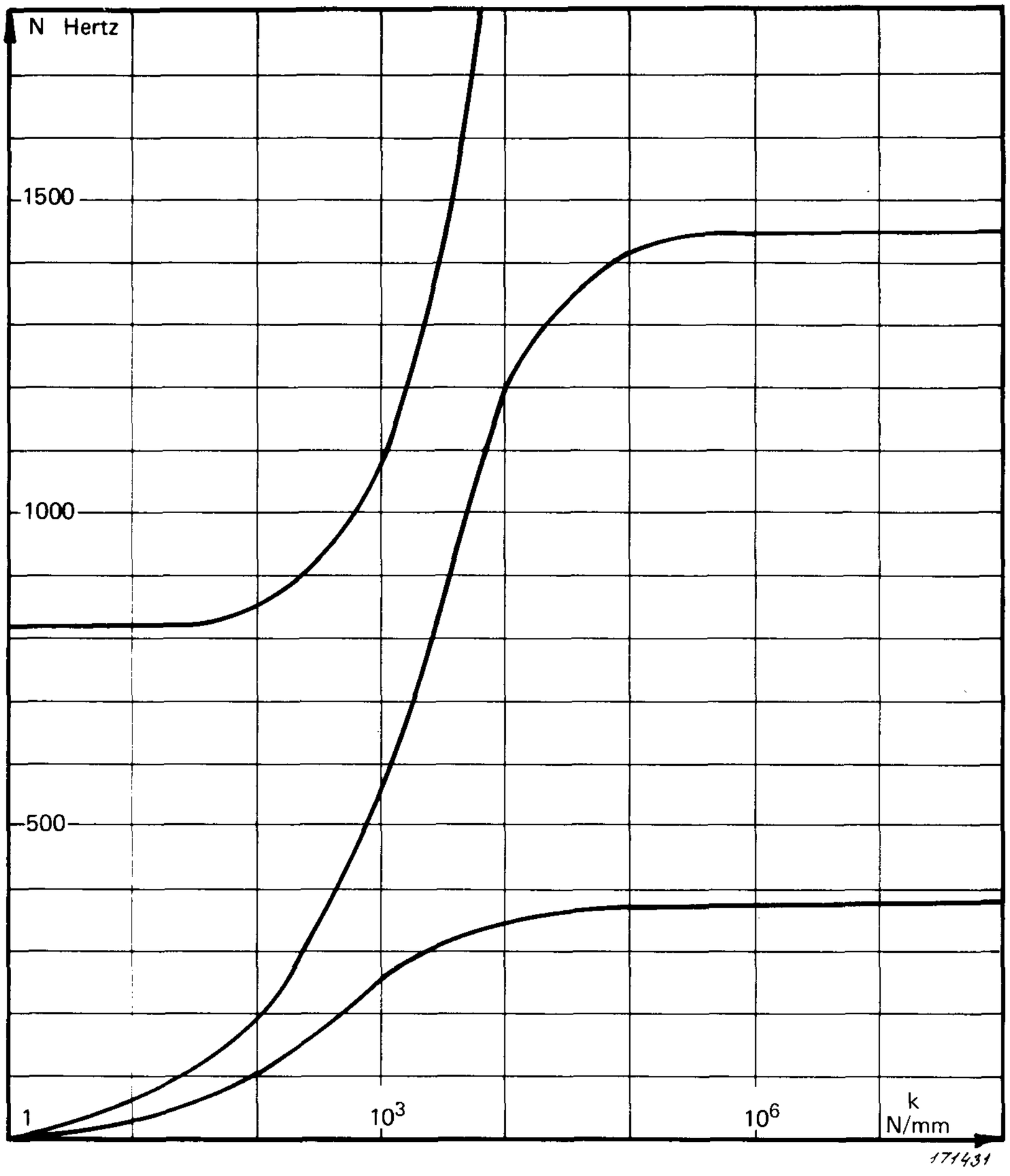

Fig.4. Natural frequencies of the beam shown in Fig.3

Fig.4 displays, in a linear frequency scale, the first three natural frequencies of a beam with length l = 0.3 m, diameter D = 0.016 m, mass density ρ = 7.8 t/m^3 and modulus of elasticity E = 21 GN/m^2.

When the value of k is varied gradually from zero to infinity, a regular change from free-free conditions to rigid support conditions can be observed. Note that for low values of support stiffness (for example k = 10 N/mm) the first two frequencies found correspond to those of a rigid rod resting on the elastic supports, namely the vertical translatory motion and the rotational motion around its centre of gravity. The ratio of the two frequencies should be 1.732 according to the mechanics of rigid bodies. In

fact it is 1.737 thereby already indicating a slight influence of deformation of the rod.

For very rigid supports, however, ($k = 10^6$ N/mm for example) their ratio is 3,99 which should be compared to the theoretical value of 3.997 given by the theory of elasticity. This example demonstrates clearly that the mechanics of rigid bodies smoothly changes to the mechanism of continuous media.

The numerical example can be extended to cover all types of beams with constant cross-section by introducing dimensionless axes as shown in Fig.5. Here the factors X_i^2 (dimensionless natural frequencies) are plotted to a logarithmic scale as functions of $(kl^3/(2\,EI)$ (dimensionless support stiffness). From the figure it can directly be seen that free-free conditions are obtained for

$$\frac{kl^3}{2EI} < 1 \tag{4}$$

Similarly, rigid support conditions are experienced for (for the first six natural frequencies)

$$\frac{kl^3}{2EI} > 10^5 \tag{5}$$

The motion of the rod was calculated for different support configurations and it was established that the effects of changing the distance between the supports and those of changing the support positions were negligible. This was confirmed by experiments. Also, different ways of obtaining the elastic support were investigated. It was found that the material used for the support (rubber, metal springs etc.) was not critical. In the extreme case of the sample resting on foam rubber, free-free conditions could still be obtained.

From the conditions stated above, it can be seen that there is a practical lower limit to the weight of the specimens which can be tested in free-free condition on account of the difficulty of achieving in this case very low stiffness supports. For very light structures, therefore, the rigid support configuration is preferable.

After selection of the support configuration, the complete equation of motion must be applied to the test sample

$$\rho S \frac{\partial^2 U}{\partial t^2} - \rho I \left(1 + \frac{E}{G\alpha}\right) \frac{\partial^4 U}{\partial x^2 \partial t^2} + EI \frac{\partial^4 U}{\partial x^4} + \frac{\rho^2 I}{G\alpha} \frac{\partial^4 U}{\partial t^4} = 0 \tag{6}$$

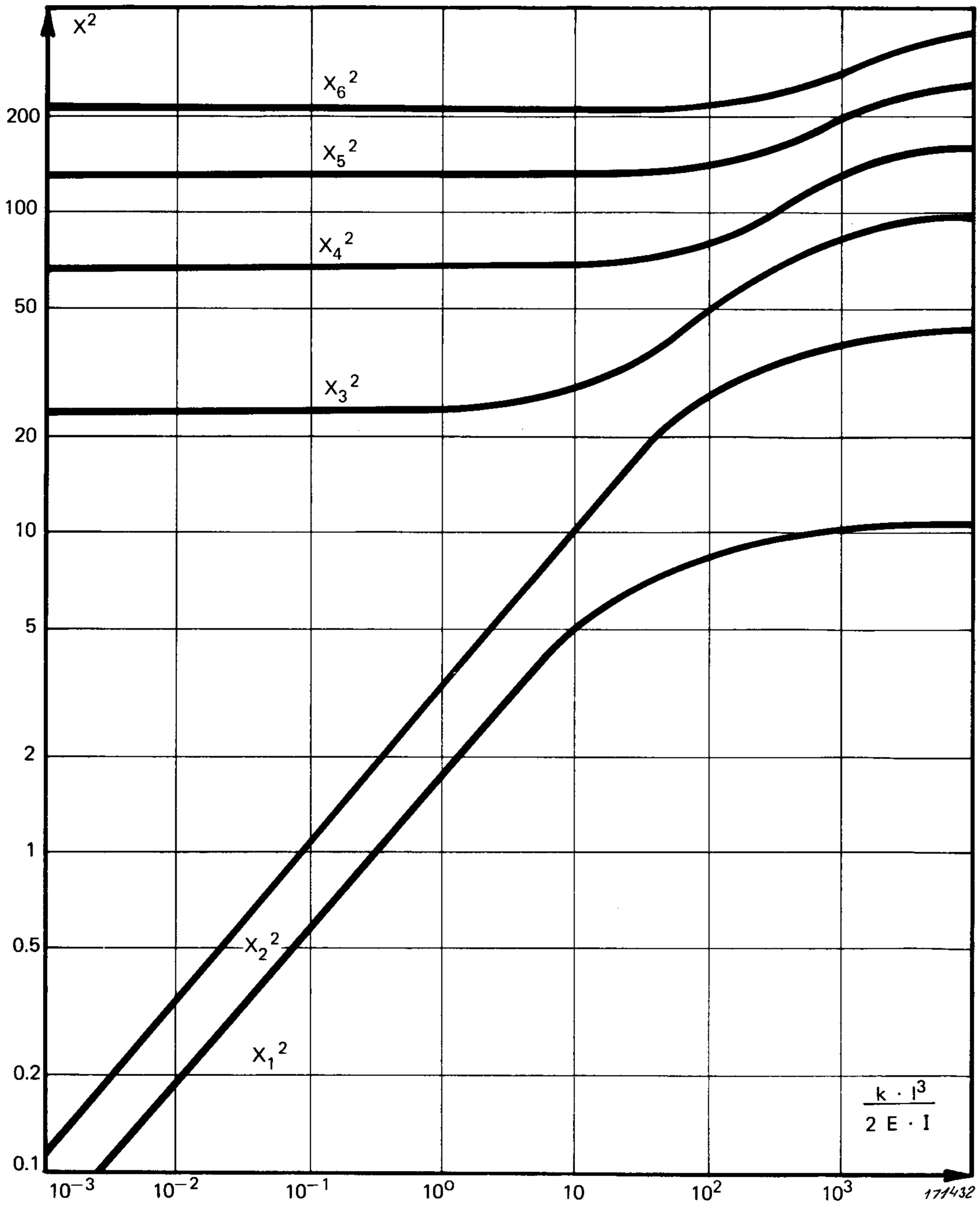

Fig.5. Dimensionless representation of natural frequencies for the beam shown in Fig.3

The solution has the form (7)

$$U(x,t) = (A \cos m_1 x + B \sin m_1 x + C \cosh m_2 x + D \sinh m_2 x) \cos (X^{*2} \sqrt{\frac{EI}{\rho S l^4}}\, t + \psi)$$

where the natural frequencies are

$$N_i = \frac{X_i^{*2}}{2\pi} \sqrt{\frac{EI}{\rho S l^4}} \tag{8}$$

and the modulus of elasticity can be obtained from

$$E = \frac{N_i^2 (2\pi)^2}{X_i^{*4}} \frac{\rho S l^4}{I} \tag{9}$$

To facilitate the calculations of E the value of X_i^{*2} has been tabulated for beams with different cross-sections. Table 1 shows the results for rods with circular cross-section.

It should be mentioned that for large ratios of l/D,

as $l/D \to \infty$,

so $X_i^{*2} \to X_i^2$

For thin strips of very limited rigidity the practical problems of measurement made it preferable, either to use more supports or, better, curved beams. The theories of those cases are not included here on account of their lengthiness.

Experimental Results

Experiments were carried out on a cylindrical rod, for which the elastic modulus was previously determined by a compression wave test to be E = 20.8 GN/m^2. The mass density was precisely measured as ρ = 7.8 t/m^2 and the theoretical form factor α = 0.9 for the cross-section was applied.

No difference was found between natural frequencies determined by experiment and those calculated from the complete equation, where shearing stresses and cross-section rotation where taken into account. The frequencies calculated from the simplified formula, however, were higher than the true values, increasing with the order of modes to a difference of 9.5% at the 5th mode (see Fig.6). The comparison on a cylindrical rod was useful to check the validity of the applied mathematical model. It was also valuable to develop the flexural wave method which has thus proved highly competitive to the compression wave method.

The method was then applied to thin tubes. The first step was to determine the form factor α experimentally. Since the modulus of elasticity is obviously independent of the flexural mode considered, each of the measured

L/D	x_1^{*2} First Mode	x_2^{*2} Second Mode	x_3^{*2} Third Mode	x_4^{*2} Fourth Mode	x_5^{*2} Fifth Mode
4.0	19.529366	45.138428	74.537180	104.207784	132.803081
5.0	20.391805	49.304525	84.178348	121.272891	158.899514
6.0	20.925556	52.163874	91.358773	134.476462	179.413131
7.0	21.274497	54.184905	96.790255	144.928896	196.144449
8.0	21.513355	55.651755	100.956934	153.293883	209.960879
9.0	21.683245	56.742032	104.197313	160.046955	221.449994
10.0	21.808012	57.570375	106.750983	165.544149	231.058152
11.0	21.902144	58.212005	108.789320	170.055760	239.136785
12.0	21.974810	58.717707	110.435860	173.788402	245.965993
13.0	22.032016	59.122500	111.780724	176.900876	251.770165
14.0	22.077823	59.451037	112.891062	179.515926	256.729629
15.0	22.115051	59.721009	113.816559	181.729210	260.989742
16.0	22.145703	59.945340	114.594911	183.615133	264.668045
17.0	22.171232	60.133628	115.254935	185.232683	267.859936
18.0	22.192716	60.293103	115.819095	186.628588	270.643149
19.0	22.210961	60.429294	116.304341	187.840210	273.081606
20.0	22.226585	60.546475	116.724607	188.897620	275.227066
21.0	22.240065	60.647994	117.090685	189.825190	277.122892
22.0	22.251775	60.736498	117.411564	190.642640	278.804904
23.0	22.262011	60.814104	117.694177	191.366636	280.302974
24.0	22.271009	60.882633	117.944292	192.010423	281.641894
25.0	22.278961	60.943233	118.166641	192.585179	282.843261
26.0	22.286023	60.997165	118.365138	193.100242	283.924520
27.0	22.292322	61.045365	118.543038	193.563449	284.900744
28.0	22.297965	61.088615	118.703065	193.981418	285.784774
29.0	22.303038	61.127565	118.847512	194.359759	286.587595
30.0	22.307617	61.162764	118.978318	194.703254	287.318642
31.0	22.311763	61.194678	119.097135	195.015992	287.986047
32.0	22.315529	61.223700	119.205370	195.301491	288.596844
33.0	22.318960	61.250169	119.304236	195.562785	289.157140
34.0	22.322094	61.274374	119.394775	195.802501	289.672258
35.0	22.324965	61.296566	119.477890	196.023175	290.146846
36.0	22.327602	61.316960	119.554366	196.226053	290.584981
37.0	22.330029	61.335746	119.624887	196.413627	290.990247
38.0	22.332267	61.353087	119.690052	196.587181	291.365805
39.0	22.334337	61.369128	119.750386	196.748066	291.714450
40.0	22.336254	61.383995	119.806354	196.897474	292.038660
41.0	22.338033	61.397799	119.858365	197.036462	292.340638
42.0	22.339686	61.410639	119.906780	197.165970	292.622348
43.0	22.341227	61.422603	119.951923	197.286834	292.885542
44.0	22.342663	61.433769	119.994081	197.399801	293.131792
45.0	22.344006	61.444205	120.033509	197.505539	293.362505
46.0	22.345262	61.453974	120.070438	197.604648	293.578950
47.0	22.346439 $\downarrow x_1^2$	61.463132 $\downarrow x_2^2$	120.105074 $\downarrow x_3^2$	197.697667 $\downarrow x_4^2$	293.782267 $\downarrow x_5^2$
48.0	22.347543	61.471727	120.137601	197.785082	293.973488
49.0	22.348581	61.479806	120.168188	197.867332	294.153544
50.0	22.349557	61.487409	120.196984	197.944813	294.323282

Table 1. Tabulated values of X_i^{*2} for free-free conditions

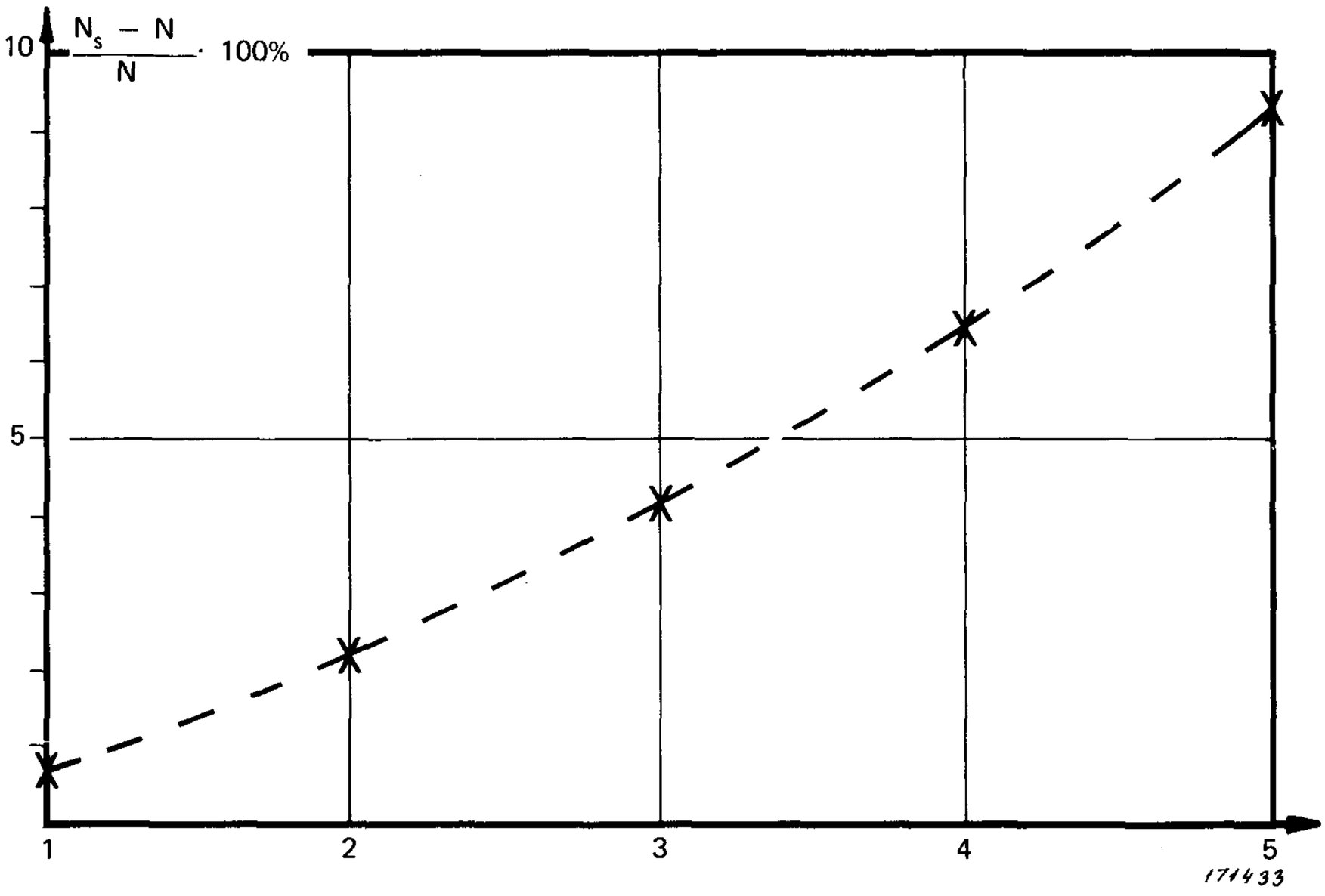

Fig.6. The difference between true natural frequencies and values calculated by the simplified formula

natural frequencies were used to calculate the modulus for different values of α around its theoretical value of 0.5. As shown in Fig.7a for the value $\alpha =$ 0.55 the modulus obtained is independent of the order of mode and equal to 18.43 GN/m^2 to an accuracy of 0.5%. This value is lower than the catalog value given by the manufacturer (20.5 GN/m^2) thereby showing the influence of the flow turning process on the elastic properties of the material (Steel NS 22 S).

For confirmation, the tube was cut to reduce its length from 800 mm to 733.5 mm. With the same form factor value the same modulus was found (Fig.7b).

Experiments were also carried out on thin strips 0.2 x 3 x 200 mm. To obtain optimal results the strips were tested in a curved configuration and Figs.8 and 9 show very clearly the first and second mode of flexural vibration respectively. Note that for the large deflections obtained on thin strips the microphone probe may be used at a larger distance than the three mm given for measurements on bars.

Measurement Apparatus

The measuring arrangement is shown in Fig.10. It consists of a Sine Random

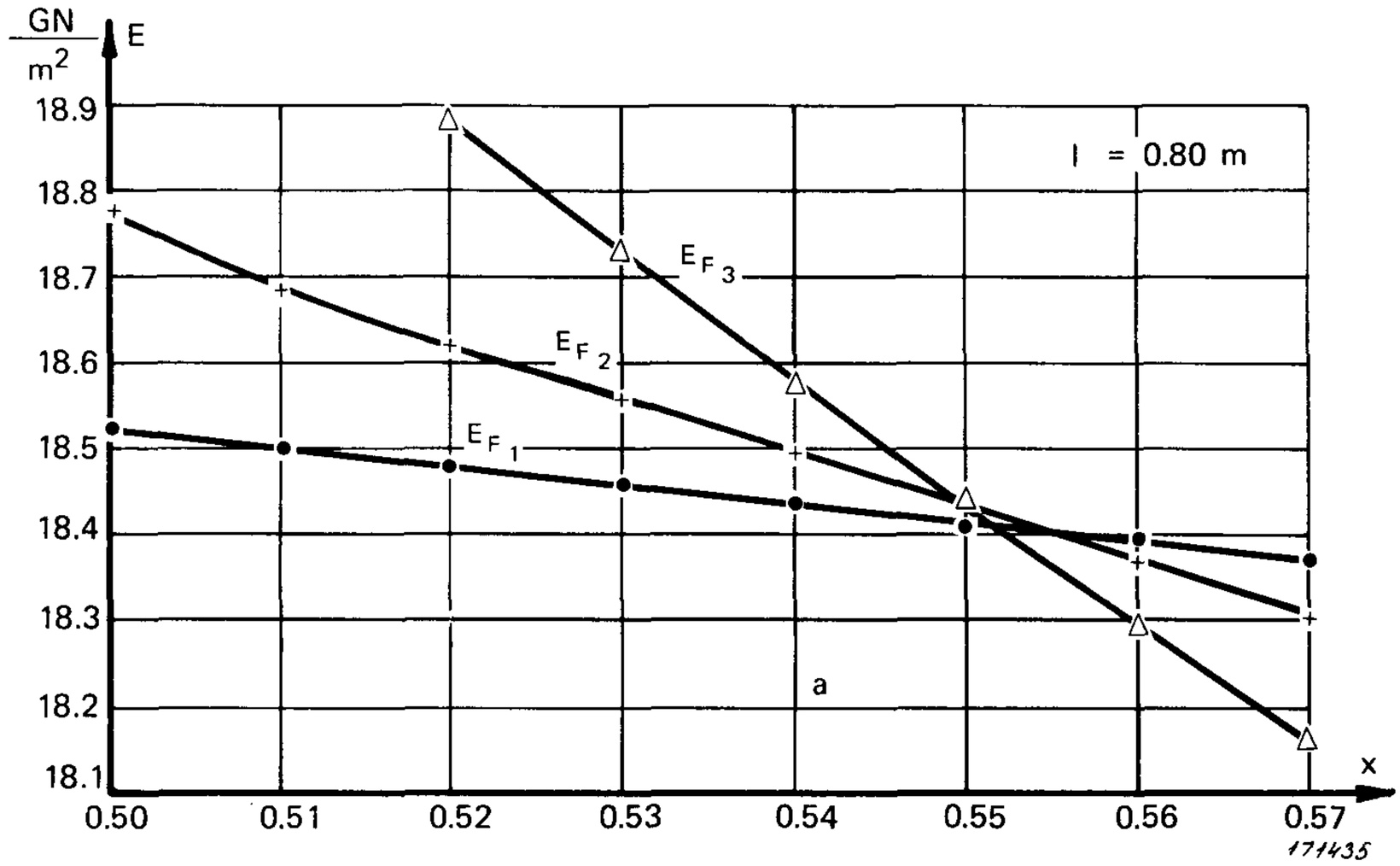

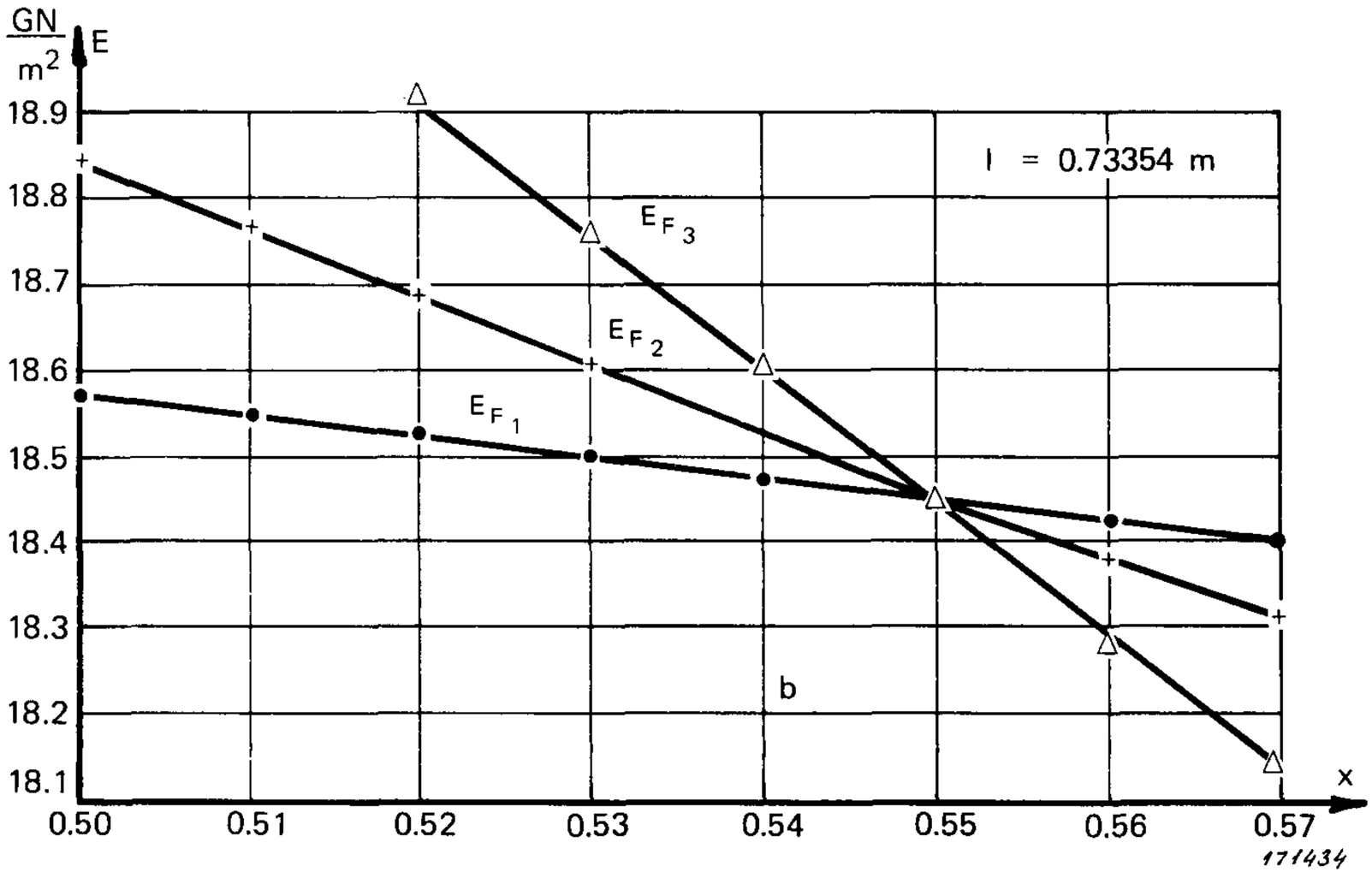

Fig.7. Determination of form factor and elastic modulus by variation of the form factor for the different modes

Generator, B & K Type 1024, which feeds a signal to the Magnetic Transducer, Type MM 0002, used to excite the structure to be tested.

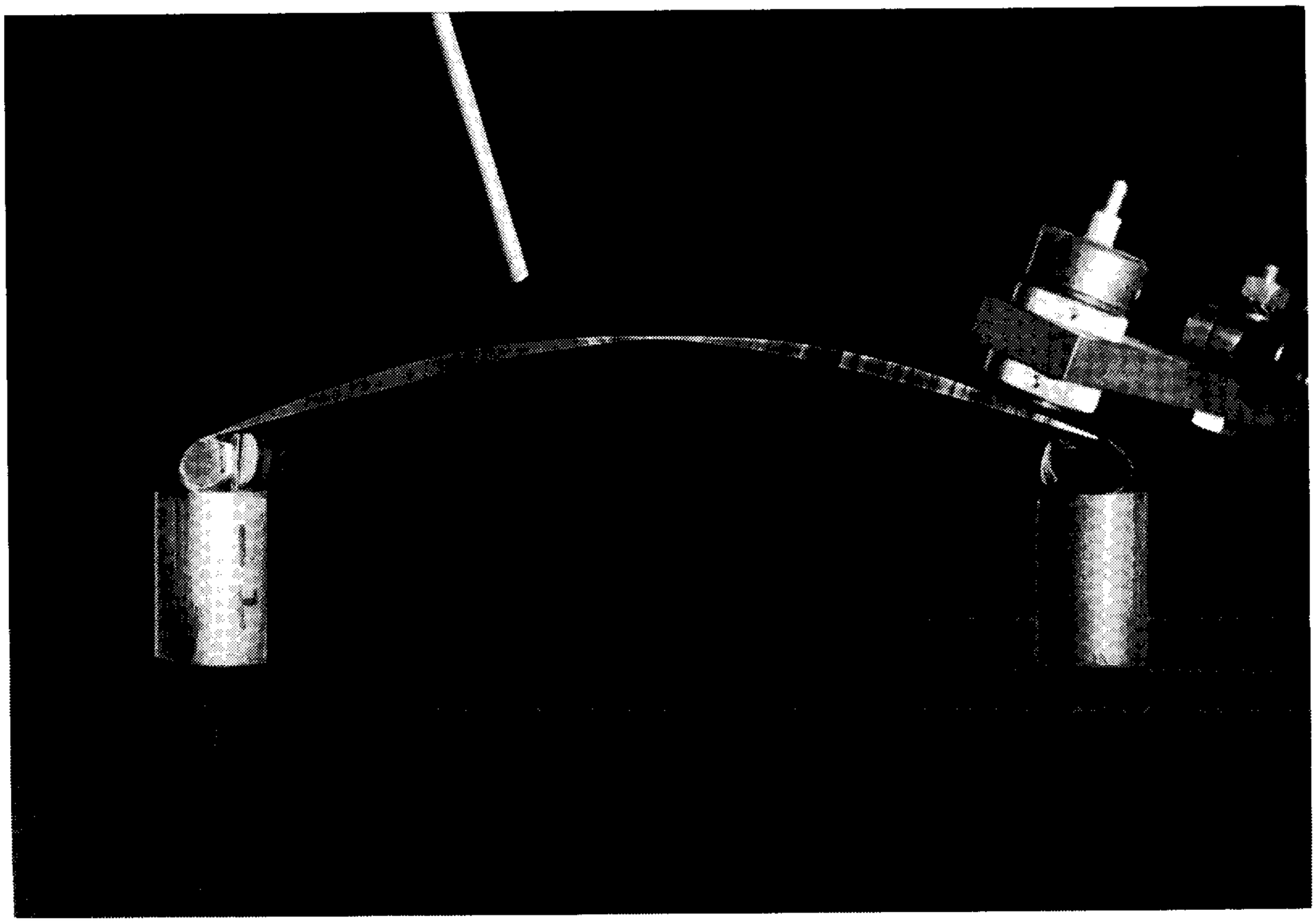

Fig.8. A curved strip experiencing the first mode of flexural vibration

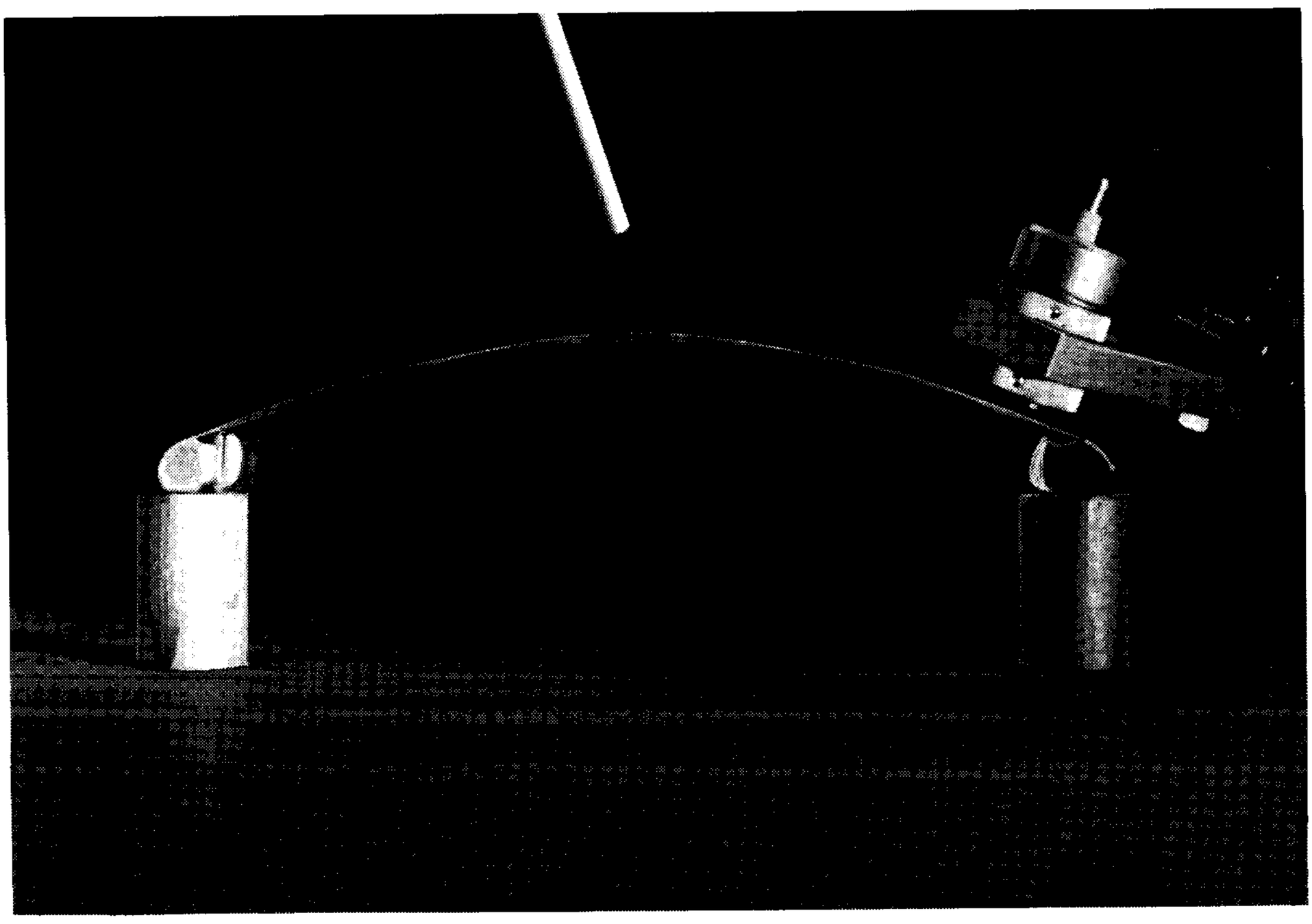

Fig.9. A curved strip experiencing the second mode of flexural vibration

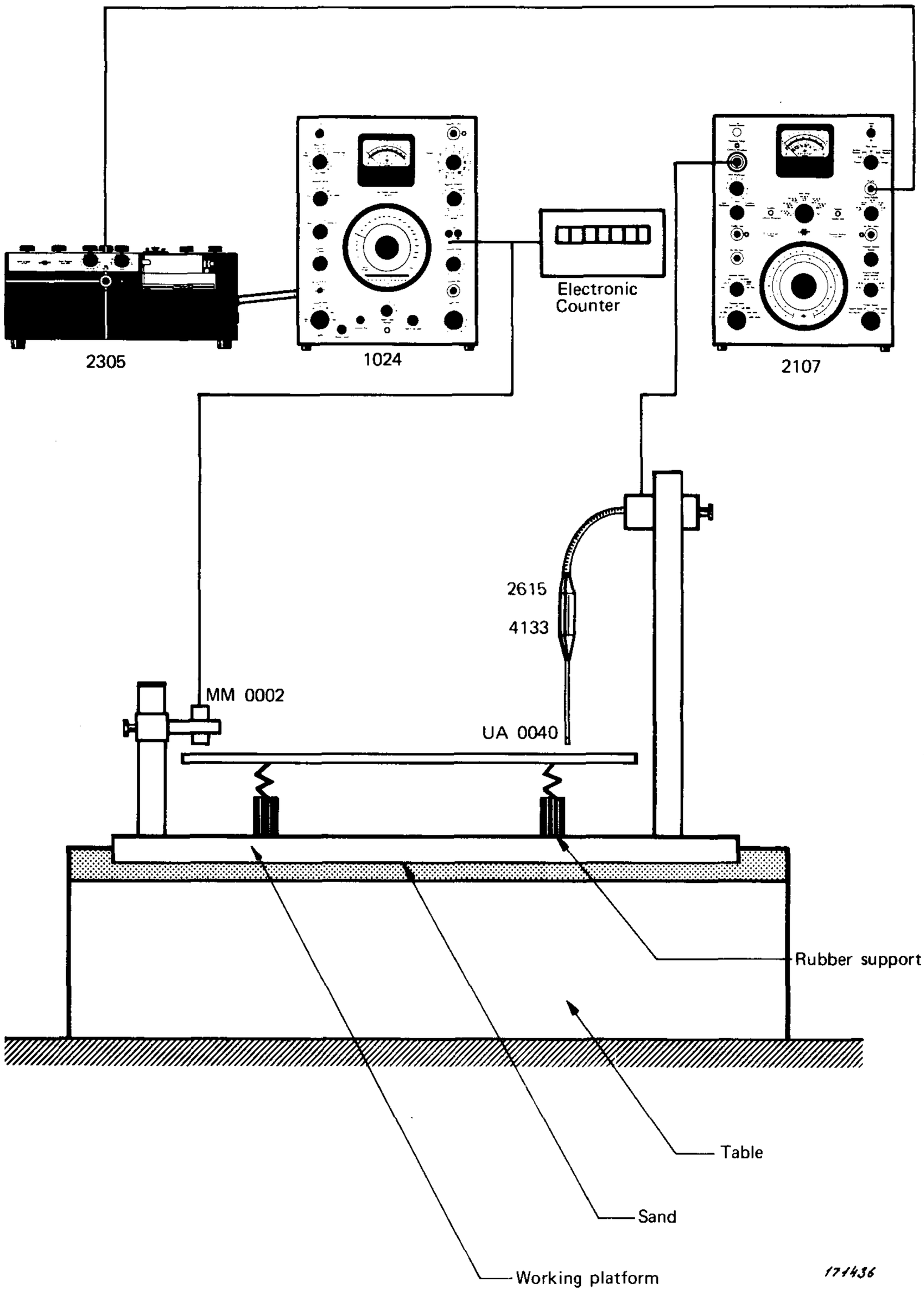

Fig. 10. The measuring arrangement

The Magnetic Transducer provides a method of exciting ferromagnetic materials without contact. For excitation of non-magnetic materials a small mu-metal pellet can be glued to the specimen or, better, a magnetic paint can be used. The exact frequency of excitation was measured by an electronic counter connected to the output of the generator.

The vibration of the specimen was detected by an acoustic transducer consisting of a 1/2" Condenser Microphone Type 4133, equipped with a Type UA 0040 Probe, the size of which was such that the vibration modes and antinodes could be determined with extreme precision. In fact, since the end of the tube was about 1 mm in diameter the position of the nodes could be determined to an accuracy of about ± 0.25 mm. Furthermore, the sound pressure level is independent of the distance from the structure to the transducer provided that it does not exceed about 3 mm.

The signal from the microphone — which is a function of the vibration level at the point of the test specimen facing the probe — is fed to a Frequency Analyzer Type 2107. Here the signal is amplified, filtered if necessary and displayed on an oscilloscope or recorded on a Level Recorder, Type 2305, the frequency of the recording paper being synchronized by mechanical means to that of the Sine Random Generator.

In order to make full use of the possibilities offered by the measuring arrangement described above, a measurement bench was designed and built to meet the required demands of overall rigidity and isolation against external vibrations. After experiments with several isolation materials (cork, rubber etc.) sand was adopted. The working platform is therefore laid and adjusted by means of a spirit-level on a bed of Fontainebleau sand about 1 cm thick.

Besides being the best vibration absorber tested, sand was also found to eliminate any deformation of the platform since the unit pressure is very small.

Measurement Technique

Both white noise and sinusoidal signals were used for excitation of the specimens. Random excitation enables the detection of all the preferential frequencies in a single measurement, the same frequencies and the same geometrical positions of the nodes and antinodes were found as in the case of sinusoidal excitation. However, the latter method has been preferred to obtain the better signal to noise ratio associated with it.

The modes of vibration were identified by measuring the vibration levels along the entire length of the specimens, taking care that the distance from the specimen to the probe tip remains constant. To facilitate the determination of the exact position of the nodes it is sometimes useful to feed the generator and transducer signals to a phase meter or to an oscilloscope to display a Lissajous figure. It is absolutely necessary to verify the mode of vibration, especially on thin shells where bending and buckling frequencies

appear together in juxtaposition, their vibration planes being perpendicular. If two of these frequencies are close together, it is almost impossible to distinguish them without a thorough exploration in the different sections.

Conclusion

The experiments have shown that, for specimens with a simple geometry which allows the formulation of exact equations, the modulus of elasticity can be found with accuracies well within 1%. Such accurate results also depend on a good choice of support stiffness, the introduction of suitable correction factors and careful realization of the experiments.

The choice of an acoustical measuring system which employs non-contact excitation and detection transducers makes it possible to disregard limitations due to the dimensions of the parts to be tested. Thereby the method allows direct evaluations of production parts.

The accurate method of determining the natural frequencies of beams, shafts etc., which is utilized with this contactless method could be very interesting to the manufacturer of high speed rotating machines, as the natural frequencies and nodes are the same in rotation and at rest (provided that the gyroscopic effects are negligible, which is generally the case).

The possibility of obtaining support stiffness between 1 N/mm and 10^4 N/mm is an extra facility in simulation of shaft conditions. It allows the adjustment of stiffness and positions for bearings – especially for shafts which will afterwards run beyond some critical frequencies.

Furthermore, the acoustical probe used has also been utilized in other applications, as for example the detection of cracks or flaws in crankshafts, since the natural frequencies will change with these faults in connection with transverse inertia.

References

P. GERMAIN: Mécanique des milieux continus.

CYRIL M. HARRIS and
CHARLES E. CREDE: Shock and vibration handbook.

S. TIMOSHENKO: Résistance des matériaux.

S. TIMOSHENKO: Théorie de l'élasticité.

Appendix

General theory for bending of constant cross-section beams

The theory is developed under the assumption that the damping of the specimen is negligible.

The fundamental formulas are: (see also Fig.A1):

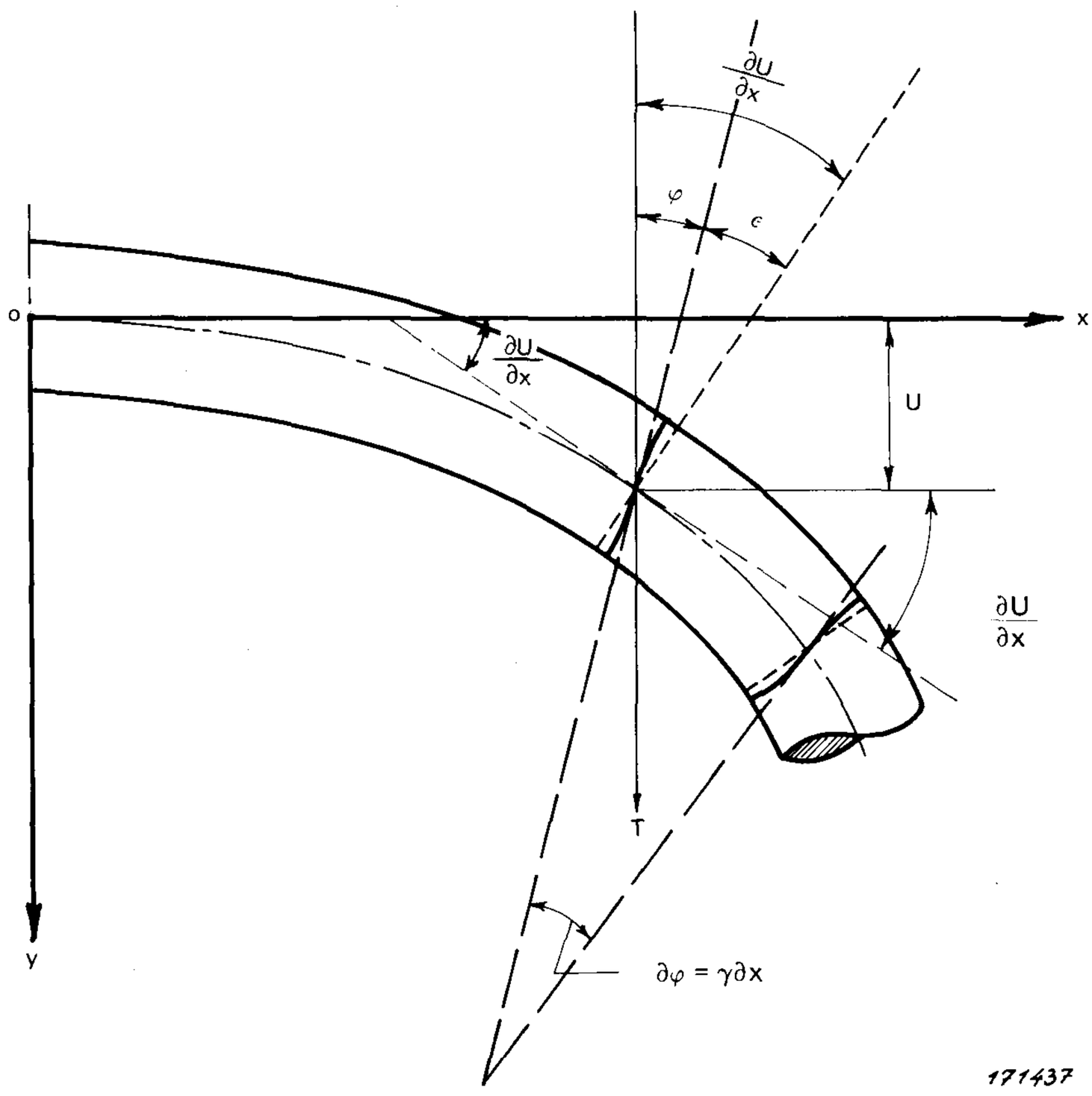

Fig.A1. The geometry of bending for a beam

The equations of motion:

$$\frac{\partial T}{\partial x} = \rho S \frac{\partial^2 U}{\partial t^2} \qquad (1)$$

$$\frac{\partial M}{\partial x} + T = \rho I \frac{\partial^2 \varphi}{\partial t^2} \qquad (2)$$

where

$T(x,t)$	is the shearing force
$M(x,t)$	is the bending moment
S	is the area of the cross-section
I	is the moment of inertia of the cross-section about an axis contained in its plane
$U(x,t)$	is the displacement along oy
$\varphi(x,t)$	is the angle of rotation of a cross-section
ρ	is the mass density of the material

The strain-displacement relations:

$$\epsilon = \frac{\partial U}{\partial x} - \varphi \tag{3}$$

$$\gamma = \frac{\partial \varphi}{\partial x} \tag{4}$$

where

ϵ	is the unit strain along oy
γ	is the unit deformation of the angle φ

The stress-strain relations

$$\frac{T}{S} = G\,\alpha\,\epsilon \tag{5}$$

$$\frac{M}{I\,\gamma} = E \tag{6}$$

where

E	is the modulus of elasticity (Young's modulus)
G	is the shear modulus
α	is a coefficient dependent on the geometry of the cross-section (form factor)

Elimination of T, M, φ, ϵ and γ from the six equations makes it possible to formulate the differential equation for the displacement $U(x,t)$ of the beam

$$\rho S \frac{\partial^2 U}{\partial t^2} - \rho I \left(1 + \frac{E}{G\alpha}\right) \frac{\partial^4 U}{\partial x^2 \partial t^2} + EI \frac{\partial^4 U}{\partial x^4} + \frac{\rho^2 I}{G\alpha} \frac{\partial^4 U}{\partial t^4} = 0 \tag{7}$$

The final solution of the equation is obtained by introducing the end conditions on either the displacements or on the external forces and moments, remembering that T and M are given by

$$T(x,t) = \rho S \int \frac{\partial^2 U}{\partial t^2}\, dx$$

$$M(x,t) = EI\left(\frac{\partial^2 U}{\partial x^2} - \frac{\rho}{G\alpha}\frac{\partial^2 U}{\partial t^2}\right) \qquad (7a)$$

By neglecting the effect of shear stress on the deformation, ϵ equals zero and α becomes infinite as T/S must have a finite value (see equation 5). Then

$$\rho S \frac{\partial^2 U}{\partial t^2} - \rho I \frac{\partial^4 U}{\partial x^2 \partial t^2} + EI \frac{\partial^4 U}{\partial x^4} = 0 \qquad (8)$$

The neglecting also of the cross-section rotation effects leads to the conventional expression for the simplified theory of beams

$$\rho S \frac{\partial^2 U}{\partial t^2} + EI \frac{\partial^4 U}{\partial x^4} = 0 \qquad (9)$$

Application of the simplified theory to beams lying on two elastic supports

It is assumed that the supports are point supports, that their damping is negligible and that their rigidity is linear.

To evaluate the natural frequencies of the beam of Fig.A2 it is necessary to divide it into three parts of length l_1, l_2 and l_3. For each of these parts the displacement U_j is given by the function

(10)

$$U_j(x,t) = \left(A_j \cos\frac{X}{l}x + B_j \sin\frac{X}{l}x + C_j \cosh\frac{X}{l}x + D_j \sinh\frac{X}{l}x\right) \cos\left(X^2\sqrt{\frac{EI}{\rho S l^4}}\, t + \psi\right)$$

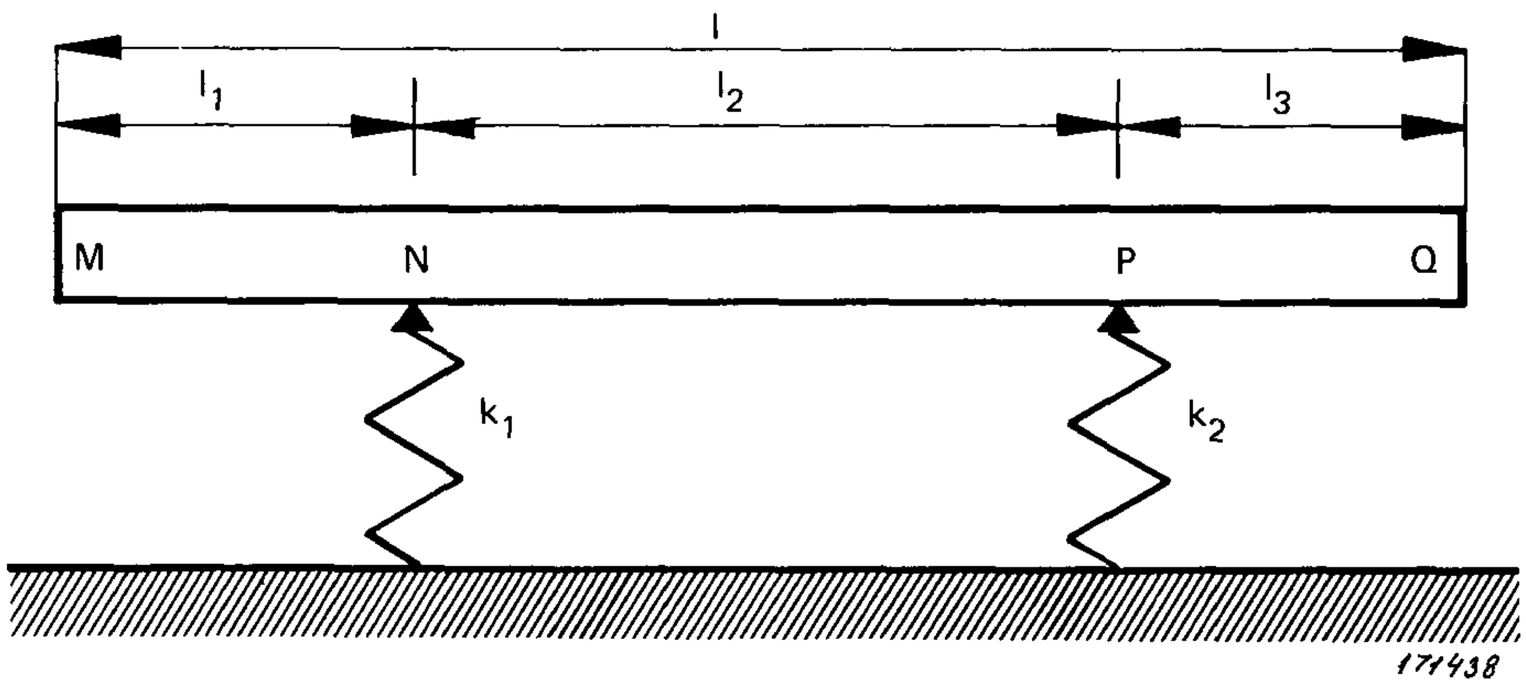

Fig.A2. A beam resting on two elastic supports

The 12 constants A_j, B_j, C_j and D_j are determined by the following end conditions (U', U'' and U''' are derivations of U with respect to x):

In M and Q the structure is free:

no moments: $$EI\, U_1''(0,t) = EI\, U_3''(l_3,t) = 0 \qquad (11)$$

no shear forces: $$EI\, U_1'''(0,t) = EI\, U_3'''(l_3,t) = 0 \qquad (12)$$

In N and P there is

equality of displacements:
$$U_1(l_1,t) = U_2(0,t)$$
$$U_2(l_2,t) = U_3(0,t) \qquad (13)$$

equality of slopes:
$$U_1'(l_1,t) = U_2'(0,t)$$
$$U_2'(l_1,t) = U_3'(0,t) \qquad (14)$$

equality of moments:
$$U_1''(l_1,t) = U_2''(0,t)$$
$$U_2''(l_1,t) = U_3''(0,t) \qquad (15)$$

discontinuity of transverse shear forces:

$$k_1\, U_1(l_1,t) - EI\, U_1'''(l_1,t) + EI\, U_2'''(0,t) = 0$$
$$k_2\, U_2(l_2,t) - EI\, U_2'''(l_2,t) + EI\, U_3'''(0,t) = 0 \qquad (16)$$

The homogeneous set of equations in A_j, B_j, C_j and D_j has a solution different from zero if its principal determinant is equal to zero. For these cases the natural frequencies N_i of the structure can be determined from the calculated coefficients X_i

$$N_i = \frac{X_i^2}{2\pi}\sqrt{\frac{EI}{\rho S l^4}} \qquad (17)$$

where

$$l = l_1 + l_2 + l_3$$

Application of the general theory (7) to the free-free beam

A particular solution of equation 7 has the following form (18)

$$U(x,t) = \left(A\cos m_1\frac{x}{l} + B\sin m_1\frac{x}{l} + C\cosh m_2\frac{x}{l} + D\sinh m_2\frac{x}{l}\right)\cos\left(X^{*2}\sqrt{\frac{EI}{\rho S l^4}}\,t + \psi\right)$$

$$
\begin{aligned}
m_1^2 &= X^{*4}\, r + \sqrt{X^{*8}\, s^2 + X^{*4}} \\
m_2^2 &= -X^{*4}\, r + \sqrt{X^{*8}\, s^2 + X^{*4}}
\end{aligned}
\qquad (19)
$$

$$
r = \frac{I}{2SI^2}\left(1 + \frac{E}{G\alpha}\right)
$$

$$
s = \frac{I}{2SI^2}\left(1 - \frac{E}{G\alpha}\right)
$$

For a free-free beam, the external forces and moments are equal to zero. Then the end conditions are

$$
T(0,t) = T(l,t) = M(0,t) = M(l,t) = 0 \qquad (20)
$$

The introduction of the end conditions results in a homogenous set of 4 equations in A, B, C and D for which there exists solutions if the determinant is equal to zero.

This leads to

$$
1 - \cos m_1 \cosh m_2 + X^{*2}\, \frac{[2(r+s)(1+X^{*4}\, s^2) - r]}{\sqrt{1 + X^{*4}(r^2 - s^2)}} \sin m_1 \sinh m_2 = 0
$$

for $m_2^2 > 0$ (21)

$$
1 - \cos m_1 \cos p_2 + X^{*2}\, \frac{[2(r+s)(1+X^{*4}\, s^2) - r]}{\sqrt{-1 + X^{*4}(r^2 - s^2)}} \sin m_1 \sin p_2 = 0
$$

(21a)

for $m_2^2 < 0;\ m_2^2 = -p_2^2$

The natural frequencies of the structure N_i correspond to the zeros of the determinant

$$
N_i = \frac{X^{*2}}{2\pi} \sqrt{\frac{EI}{\rho S l^4}} \qquad (22)
$$

Estimation of Sound Pressure Levels at a Distance from a Noise Source

by

K. Zaveri

ABSTRACT

The article describes one of the uses of Sound Power data in determining the sound pressure level perceived at a distance from a noise source, in a Semi-Reverberant Environment. A practical example is included to illustrate the accuracies achievable.

SOMMAIRE

Cet article décrit une des utilisations de données sur la Puissance Acoustique pour déterminer le niveau de pression sonore reçu a une certaine distance d'une source de bruit, dans un environnement semi-réverbérant. On a inclus un exemple pratique pour donner une idée de la précision que l'on peut obtenir sus le résultats.

ZUSAMMENFASSUNG

Eine der Anwendungen von Schalleistungsdaten zur Bestimmung des Schalldruckpegels in der Umgebung einer Schallquelle in einem halbhalligen Raum wird beschrieben. Ein praktisches Beispiel illustriert die erreichbaren Genauigkeiten.

One of the objectives for determining sound power data, as outlined in the ISO Recommendation R 495 is to estimate the noise received at a distance from a sound source. The sound pressure level perceived at a point in a room is made up of direct sound from the source to the listener and reverberant sound arriving after one or more reflections from the room surfaces. The direct sound is a function of the directivity factor of the sound source and the distance from the listener, while the reverberant sound is a function of the room constant only. The mathematical relationship between the sound power P and sound pressure p in a large semi-reverberant room is given by the equation

$$20 \log_{10} \left(\frac{p}{p_o}\right) - 10 \log_{10} \left(\frac{P}{P_o}\right) = 10 \log_{10} \left(\frac{Q}{4\pi r^2} + \frac{4}{R}\right) \qquad (1)$$

where

p_o is the ref. sound pressure 2×10^{-5} N/m^2
P_o is the ref. sound power 10^{-12} Watts
R is the room constant and
Q is the directivity factor

The room constant R gives a measure of the sound absorption quality of the room and is mathematically defined by

$$R = \frac{S\alpha}{1-\alpha} \qquad (2)$$

where

S is the total area of the room surface

and

α is the average energy absorption coefficient of the room.

The directivity factor Q is the ratio of the intensity on a designated axis of a sound source at a specified distance r and frequency band, to the intensity that would be produced at the same position by a non-directional point source radiating the same power. If the sound source is assumed to be non-directional, Q takes the values 2, 4 and 8 when the source is placed on a hard surface (floor) in the middle of a room, on an edge between two hard surfaces, and in a corner of three hard surfaces respectively. Although these figures are somewhat rough estimates, not regarding the detailed radiation characteristics of the sound source, they may serve as useful guides for practical estimation purposes at low frequencies.

The physical meaning of expression (1) can best be appreciated with the aid of Fig.1. The quantity $10 \log_{10} \left(\frac{Q}{4\pi r^2} + \frac{4}{R}\right)$ is plotted as the ordinate against the distance r from the sound source in meters. The curves are plotted with various values of the room constant R in square meters as a parameter and with values of directivity factor Q greater than unity. From the above equation it can be seen that for a specific room constant and directivity factor, the sound pressure level at a distance r is given by the sum of the ordinate and the sound power level. The condition for $R = \infty$ (complete sound absorption) and $Q = 1$, corresponds to the free suspension of a non-directional source in open air (acoustic free-field conditions).

To illustrate the use of the curves consider an arbitrary case where $R = 500\ m^2$ and $Q = 2$. From the curve it is seen that the pressure level at a distance of 2 meters from the source is practically the same as it would be if the room was not there. (The difference is less than 1 dB). The sound pressure would, however, be roughly the same in all positions in the room at a distance greater than 5 meters from the source. Therefore a machine operator standing very close to a machine will draw very little advantage from making the room more absorbent, (i.e. increasing R) but a worker at a

distance will experience a reduction of 3 dB sound pressure level for each doubling of the room constant R. It should also be noted that the parts of the curves determined by the reverberant sound field are nearly independent of Q. It is obvious, however, that the direct sound field extends to a greater distance, the greater the value of Q.

In order to make practical use of the curves it is necessary to determine the room constant R, before an estimate of the sound pressure level can be predicted. By measurement of the reverberation time T and use of equation

$$R = \frac{V}{\frac{T}{0.16} - \frac{V}{S}} \qquad (3)$$

the room constant can be determined. V is the volume in m^3 and S the surface area of the room in m^2.

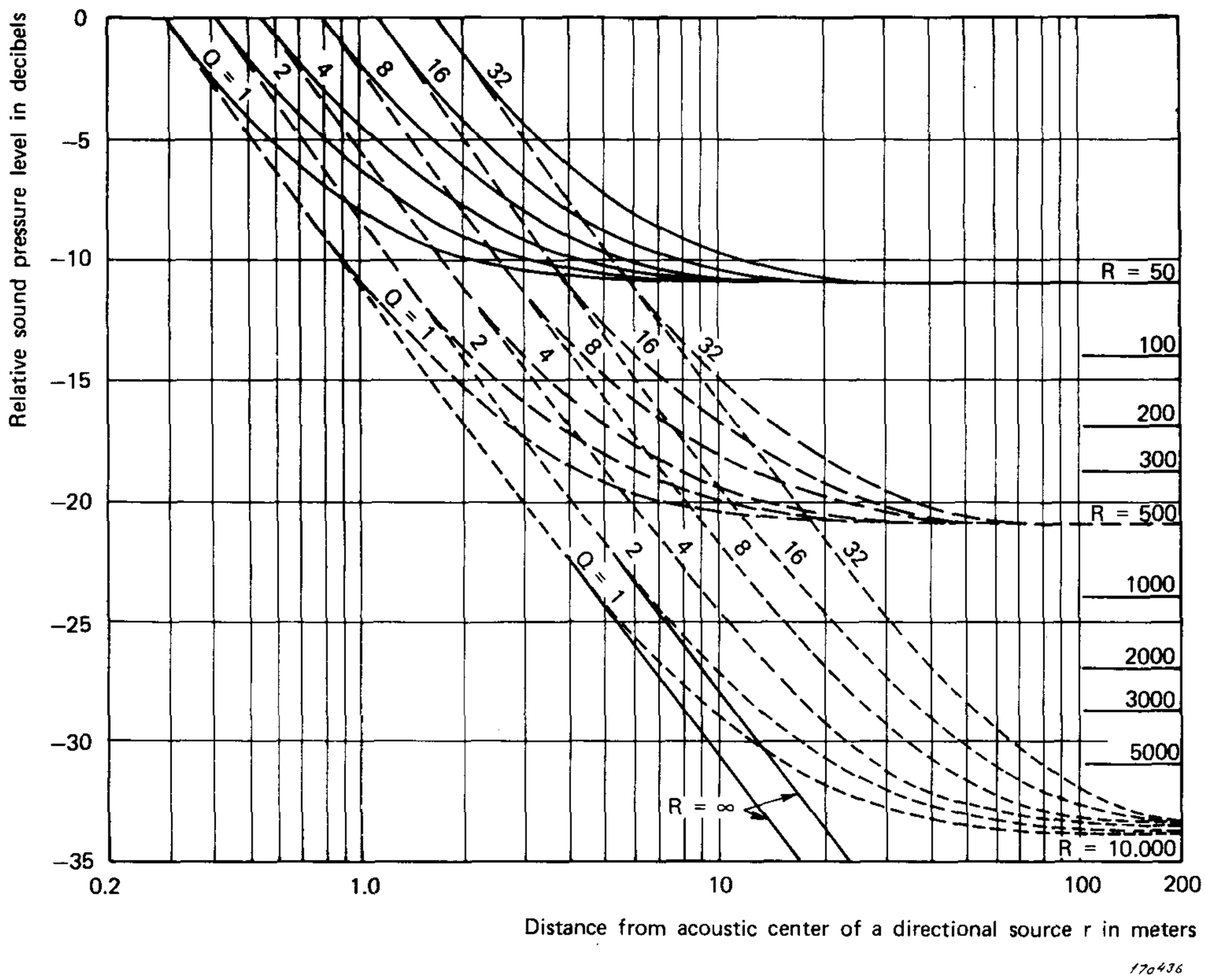

Fig. 1. Chart for determination of the sound pressure level in a large room as a function of the distance from the sound source. The room constant R, and the directivity factor Q are plotted as parameters

To exemplify the procedure an industrial type vacuum cleaner was placed in the centre of a room of surface area 310 m^2 and volume 330 m^3. The measuring arrangement used is shown in Fig.2. Measurements were made both at a distance of 2 m from the cleaner, and at a considerably larger distance away. Referring to Table 1 it can be seen that the room constant, R, varies with frequency between 57 m^2 at 125 Hz to 234 m^2 at 8 kHz.

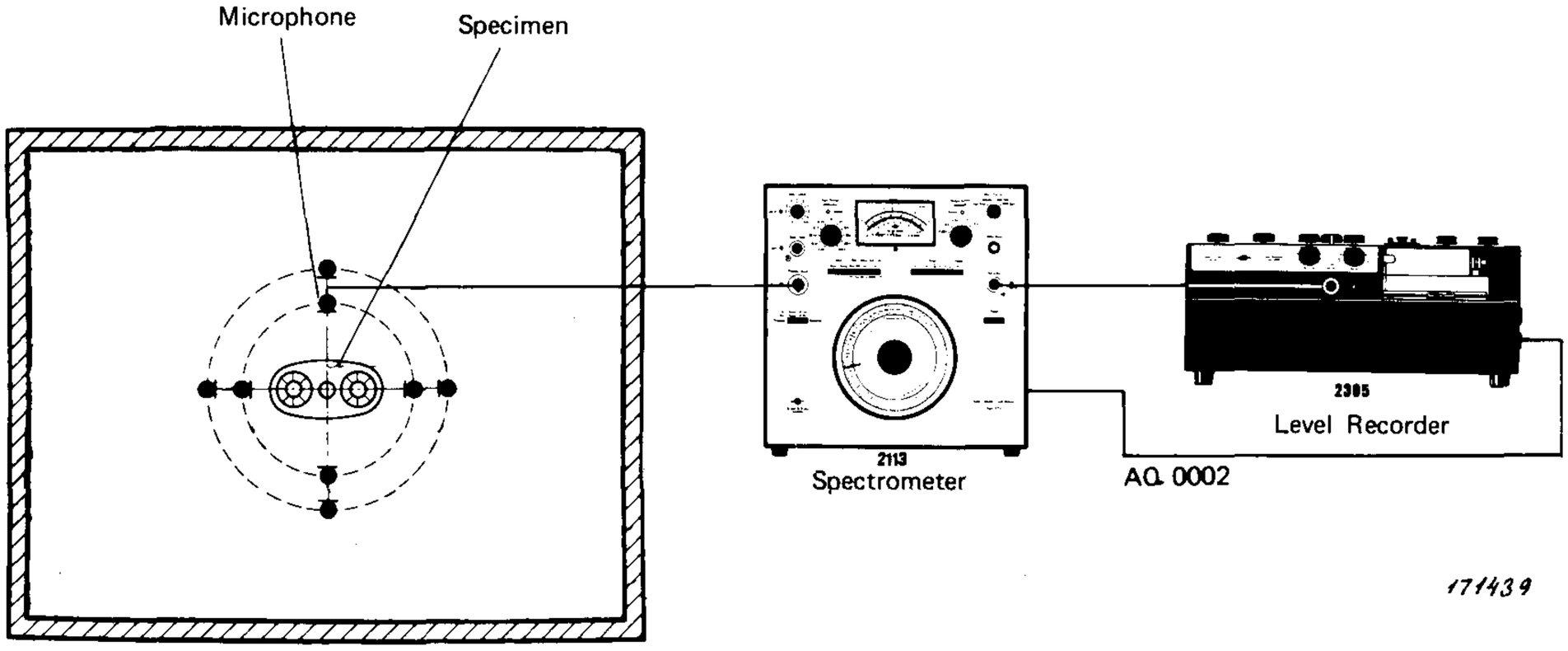

Fig.2. Measuring arrangement employing Audio Frequency Spectrometer Type 2113

Table 1. Measured and Estimated Sound Pressure Levels in a Room.

Centre Frequency of octave Band Hz	Reverberation Time T Sec.	Room Constant $R = \frac{V}{\frac{T}{0.16}\frac{V}{A}}$ m^2	Sound Power dB	Sound Pressure Level in "Free" Field = Sound Power + $+ 10 \log_{10} (\frac{2}{4 \pi r^2} + \frac{4}{R})$	Measured Mean Sound Pressure Level in "Free" Field (2 m)	Evaluated SPL - Measured SPL	Sound Pressure Level in Rever. Field = Sound Power + $+ 10 \log_{10} (\frac{4}{R})$	Measured Mean Sound Pressure Level in Rever. Field	Evaluated SPL - Measured SPL
125	1.1	57.2	74.1	64.5	62.7	1.8	62.5	60	2.5
250	0.8	84.6	74.1	63.5	64.1	− 0.6	60.6	62	− 1.2
500	0.7	100	74.3	63.3	64.2	− 0.9	60.3	61.5	− 1.2
1000	0.5	162	76.8	64.9	65.4	− 0.5	60.7	62	− 1.3
2000	0.5	162	78.1	66.2	66.3	− 0.1	62.0	62.7	− 0.7
4000	0.5	162	72.3	60.4	59.8	0.6	56.2	55.7	0.5
8000	0.4	234	63.3	50.9	52.5	− 1.6	45.6	48.3	− 2.7

Table 1. Measured and Estimated Sound Pressure Levels in a Room

By consulting Fig.1, it is found that the sound field 2 m away from the cleaner is somewhat between an acoustic free field and a reverberant field. Also, the sound field at a "considerably larger" distance away may be considered a fully reverberant field.

The results of both series of measurements are given in the table and compared to estimated sound pressure level values. It should be noted that a directivity factor of Q = 2 has been used in the estimation procedure, due to the position of the vacuum cleaner on the floor in the centre of the room. By comparing the measured and estimated values of the sound pressure levels an idea about the accuracy that is to be expected from these kind of estimations is obtained. It can be seen that estimation errors of the order ±2 dB (or larger) may be present. The accuracy could be improved if knowledge of the directional characteristics of the sound source was available. However, the directivity should not be highly pronounced.

One other requirement, as mentioned above, is that the enclosure should not be too small, as it would react on the sound source to modify its radiated power. The room can be considered large enough if the mean free path is several wavelengths long. It is also advantageous if the room is irregular in shape and contains objects such as tables, chairs, cabinets, etc., which is often the case met in actual practice.

Before finishing this brief discussion on sound pressure level estimations it should be mentioned that the sound pressure level close to a hard surface, or in a corner, is normally somewhat larger than that predicted for the fully reverberant field. This is due to concentrations of reflections, and in a corner the sound pressure level might be as much as 9 dB larger than the reverberant field value. Typical increase in octave band values measured for the case of broadband acoustic noise are shown below.

Centre freq. (Hz)	125	250	500	1000	2000	4000
S.P.L. increase	6 dB	6,5 dB	7,5 dB	7 dB	6,5 dB	3 dB

References:

BERANEK, L.L.: Acoustics. McGraw Hill Book Co., Inc. 1954.

BERANEK, L.L.: Noise Reduction. McGraw Hill Book Co., Inc. 1960.

BROCH, J.T.: Acoustic Noise Measurements, Brüel & Kjær 1971.

ZAVERI, K.J.: Conventional & On-line Sound Power Measurements, Brüel & Kjær "Technical Review" No. 3, 1971.

Brief Communications

The intention of this section in the B & K Technical Reviews is to cover more practical aspects of the use of Brüel & Kjær instruments. It is meant to be an "open forum" for communication between the readers of the Review and our development and application laboratories. We therefore invite you to contribute to this communication whenever you have solved a measurement problem that you think may be of general interest to users of B & K equipment. The only restriction to contributions is that they should be as short as possible and preferably no longer than 3 typewritten pages (A 4).

Acoustical Calibrator Type 4230 and its Equivalent Diagram*)

by

Erling Frederiksen

One of the newer instruments in the Brüel & Kjær program is an Acoustical Calibrator Type 4230 (Fig.1) which produces a sound pressure of 1 N/m^2 (94 dB ref. 2×10^{-5} N/m^2) at 1000 Hz. One remarkable property of the calibrator is that it is virtually insensitive even to large changes in atmospheric pressure.

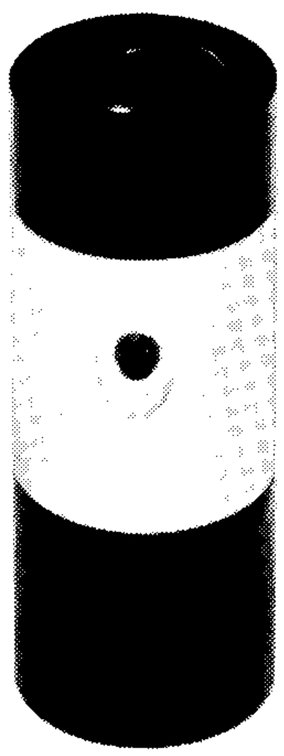

Fig.1. Sound Level Calibrator, Type 4230

*) Paper presented at "Nordic Acoustic Meeting", Copenhagen, 24.–26. August, 1970.

Another advantage of this calibrator is that in spite of its small outer dimensions, it has a large equivalent coupler volume which renders the sound pressure independent of varying cavities and equivalent volumes of the microphones mounted on it. These desirable properties were obtainable on account of establishing equivalent electrical diagrams for mechanical, electrical and acoustical systems in the early design stage. The equivalent circuits made it possible to measure or calculate the influence of individual elements on the properties of the calibrator, which could be optimized for example with respect to temperature and atmospheric pressure.

A cross-sectional view of the calibrator is shown in Fig.2. It consists of a Zener stabilized oscillator which delivers current via a potentiometer to a piezoelectric crystal. The crystal is soldered onto a metallic suspension system, which is designed so that its influence on the stiffness of the crystal is minimized. The force generated by the crystal is transformed by a conical nickel-membrane to a sound pressure in the coupler to which the microphone is subjected.

The conical part of the membrane forms a stiff piston while the plane edge of the membrane is elastic. To obtain low acoustic impedance from the point of view of the coupler volume, the moving mechanical parts of the system are adjusted to resonate at 1000 Hz which is the signal frequency of the calibrator. Since the mass and stiffness of the membrane and crystal would give a higher resonant frequency, the frequency can be lowered by adding a mass to the membrane.

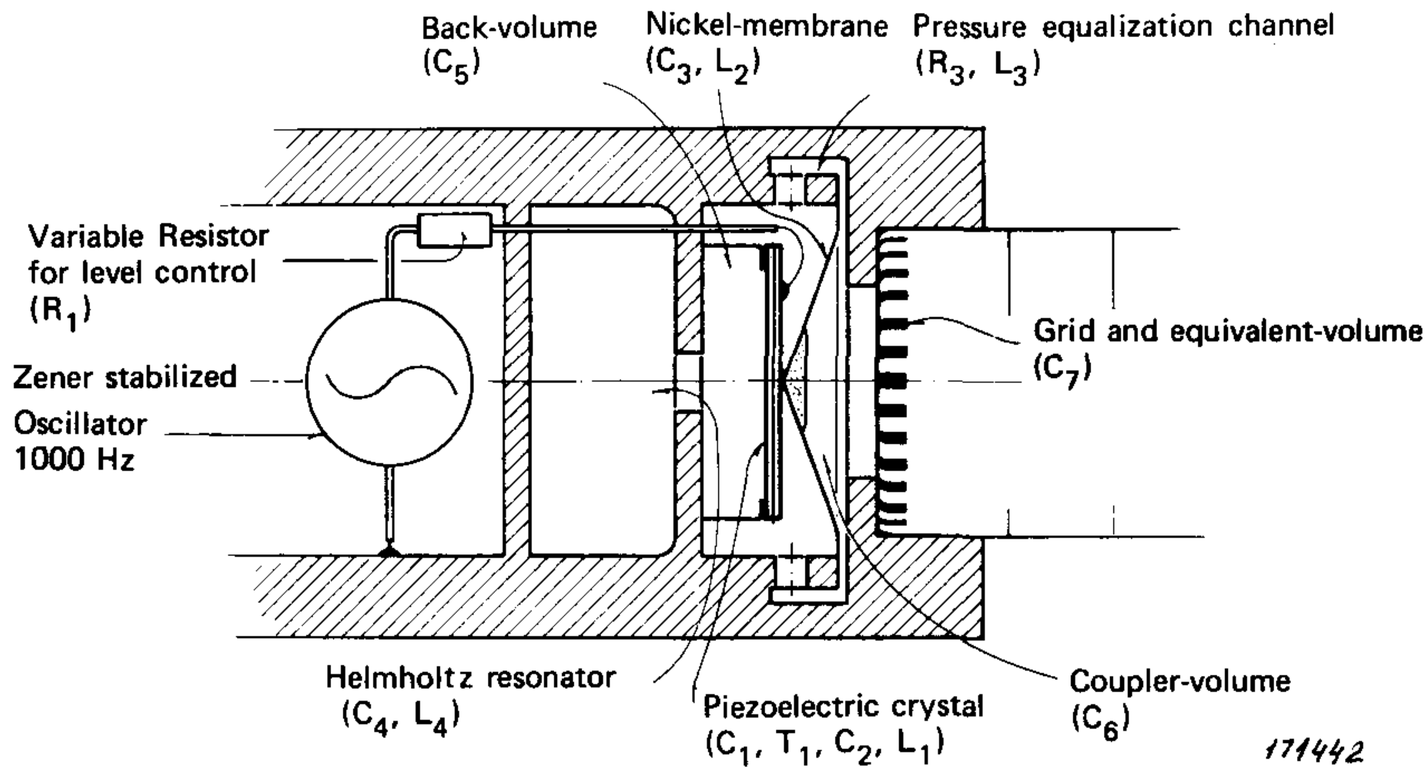

Fig.2. Cross-sectional view of the calibrator

It is desirable to eliminate the cavity stiffness behind the membrane since it changes in proportion to the atmospheric pressure and would therefore influence the resonant frequency of the system. This is achieved by coupling a Helmholtz resonator (with resonant frequency 1000 Hz) whereby a very low acoustic impedance is obtained at this frequency.

Finally, a pressure equalization canal between the coupler and the cavity behind the membrane is incorporated in the calibrator, to reduce the large pressure variations caused by "piston" effects, when microphones are coupled on and off, which could otherwise damage both the calibrator and the microphones.

An equivalent circuit for the above mentioned elements is shown in Fig.3.

The impedance analogy has been used, i.e. mechanical or acoustic mass is replaced by an inductance, compliance (1/stiffness) by capacity, and damping by electrical resistance. The dimensions of the single elements are determined partly by calculation and partly by transferring the given mechanical and electrical data of the crystal to acoustical units, taking into consideration the area of the membrane through which the real acoustical elements are coupled.

For actual build-up of the circuit in practice, the generating side of the circuit is modified whereby the transformer can be omitted, and the impedances of the electrical elements are reduced by a factor of 10^3 to obtain the order of component impedances met in actual practice.

The equivalent circuit diagram which is reduced to the one shown in Fig.4, is valid for an atmospheric pressure of 760 mm of Hg. Similar circuits have also been built for lower static pressures. For doing so, the reactance of the acoustic elements has been changed in proportion to the pressure reduction.

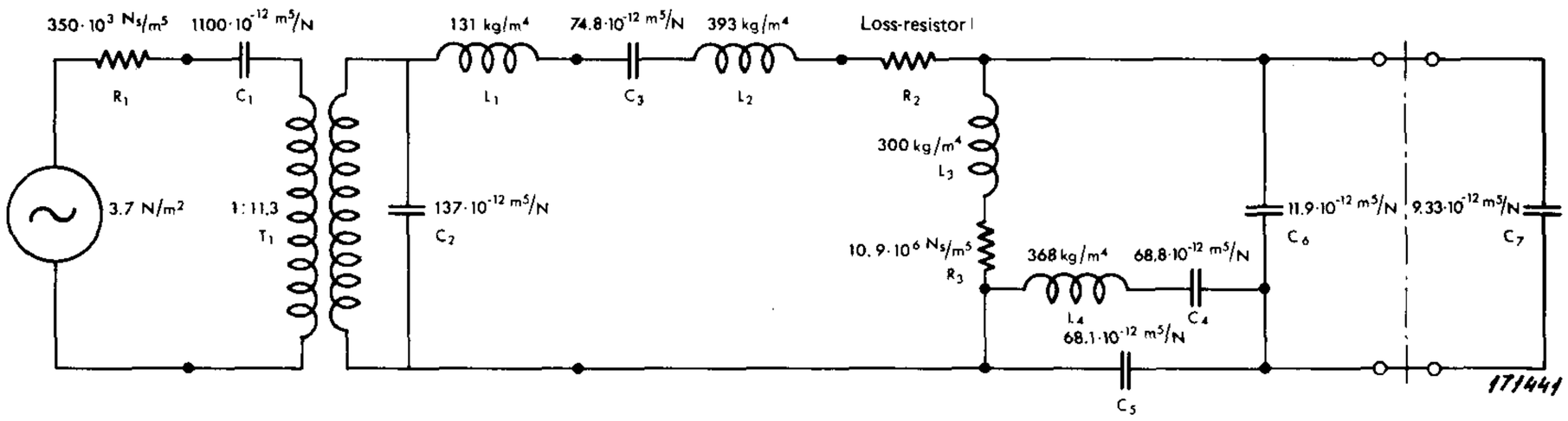

Fig.3. Electrical equivalent circuit diagram (for 1013 mbar, 25°C)

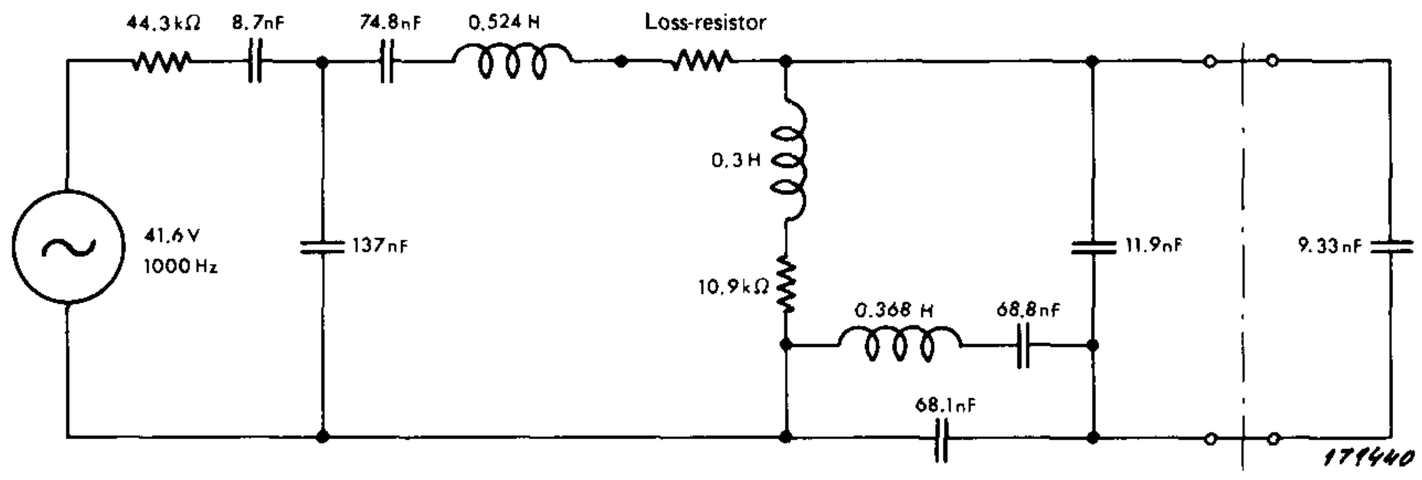

Fig.4. Reduced equivalent circuit diagram

Fig.5 shows the equivalent volume as a function of frequency measured on a typical calibrator and on the electrical model. Apart from minor differences due to the spread in parameters, there is generally good agreement over most of the frequency range.

The slight difference in the slope of the curves at low frequencies is caused by ignoring in the electrical model leaks in the coupler thread.

Equivalence of the two systems cannot be expected over 5 kHz on account of the resonances occuring in individual mechanical and acoustic elements.

Fig.6 shows the sound pressure measured as a function of frequency for the calibrator and the electrical model. Here again the curves agree remarkably uptil 5 kHz. The characteristics of the model show that the sound pressure level is not influenced by the atmospheric pressure at 1000 Hz. Corresponding measurements on the calibrator are shown in Fig.7, where both the axes are considerably enlarged to give a better resolution at 1000 Hz.

No attempt has been made to determine other loss resistances than those shown in the diagram. The series loss resistance, which is the internal resistance of the calibrator at 25°C can be determined, either directly by impedance measurements, or it can be determined by measurements as shown in Fig.7, where the static pressure is determined for a given fall in sound pressure. Knowing the static pressure and the loading volume, the internal resistance can be calculated. A part of it originates from the electrical series resistance, which can be determined to be equal to approx. 38×10^3 Ns/m^5, while the remainder, roughly 60×10^3 Ns/m^5 is distributed over the mechanical and acoustic elements. By further reducing the static pressure, it might be possible to eliminate the acoustic elements, as the volume behind the membrane would short circuit the series loss resistance of the Helmholtz resonator, whereby the loss of the mechanical system could be determined by measuring its Q value.

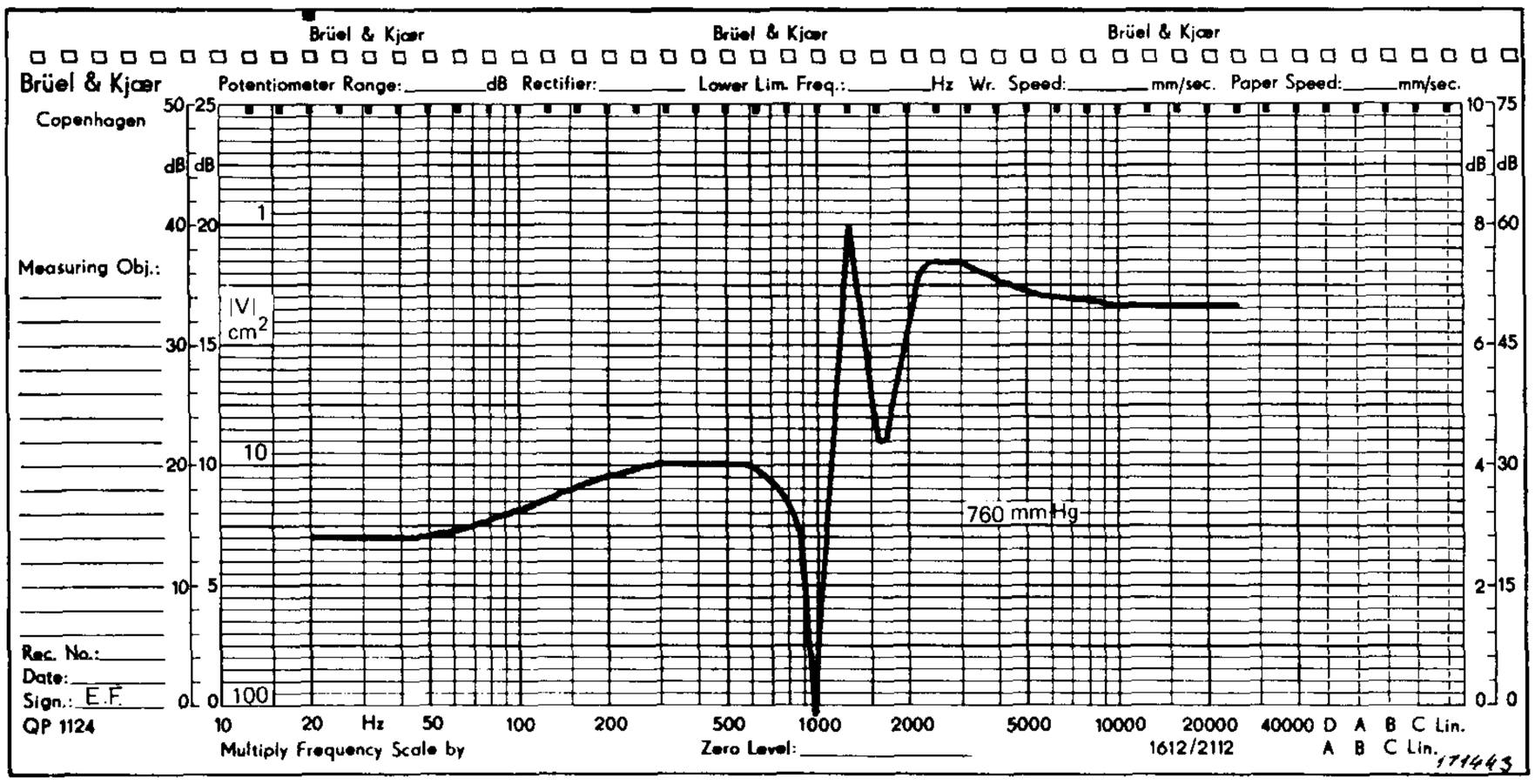

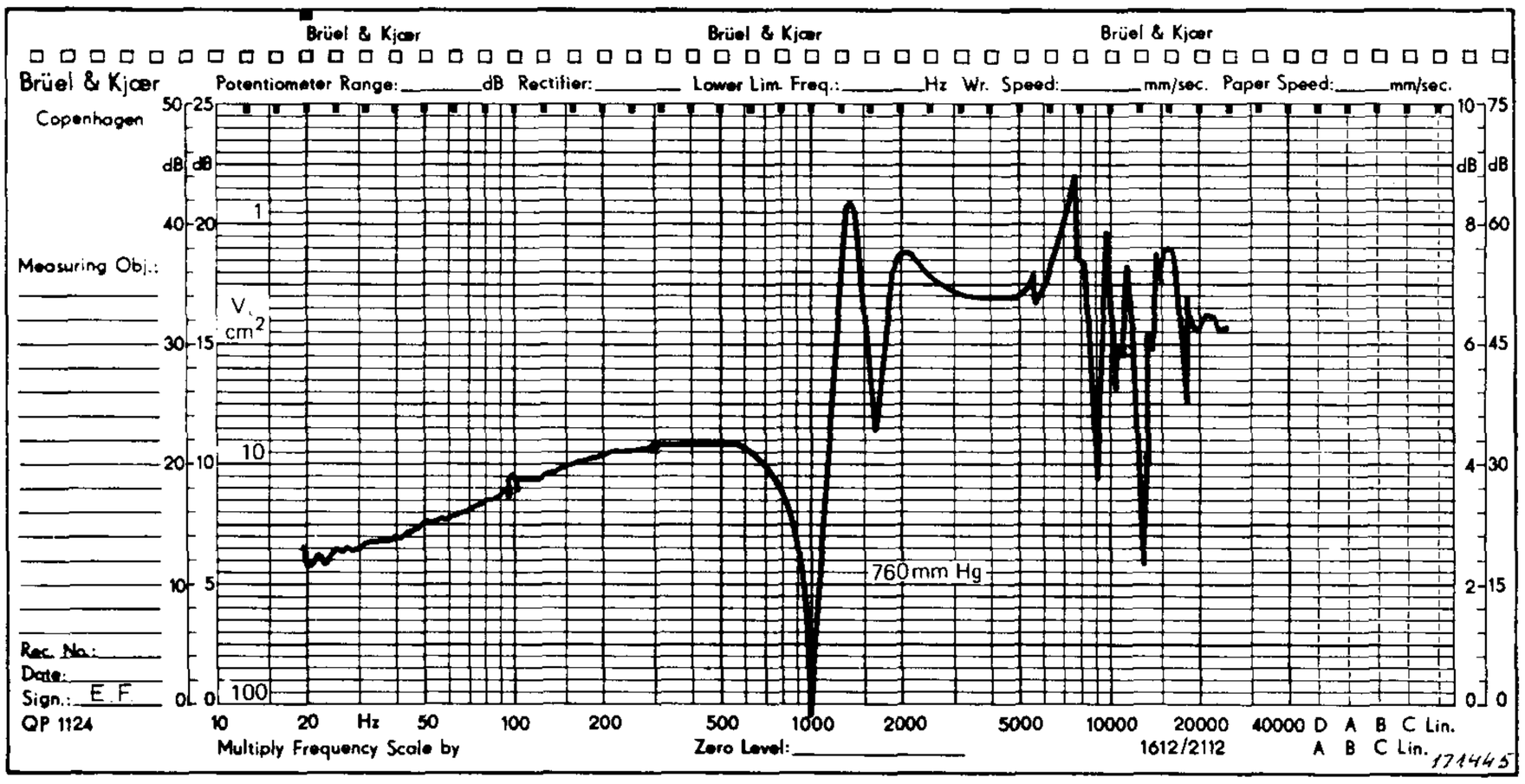

Fig.5. The equivalent volume measured as a function of frequency.
a. For the equivalent circuit
b. For the calibrator

The use of the equivalent circuit has made it feasible to analyze the function of the calibrator by electrical measurements and by numerical evaluations. Under all circumstances, it is important that the functioning of the instrument is fully understood before it is set into production.

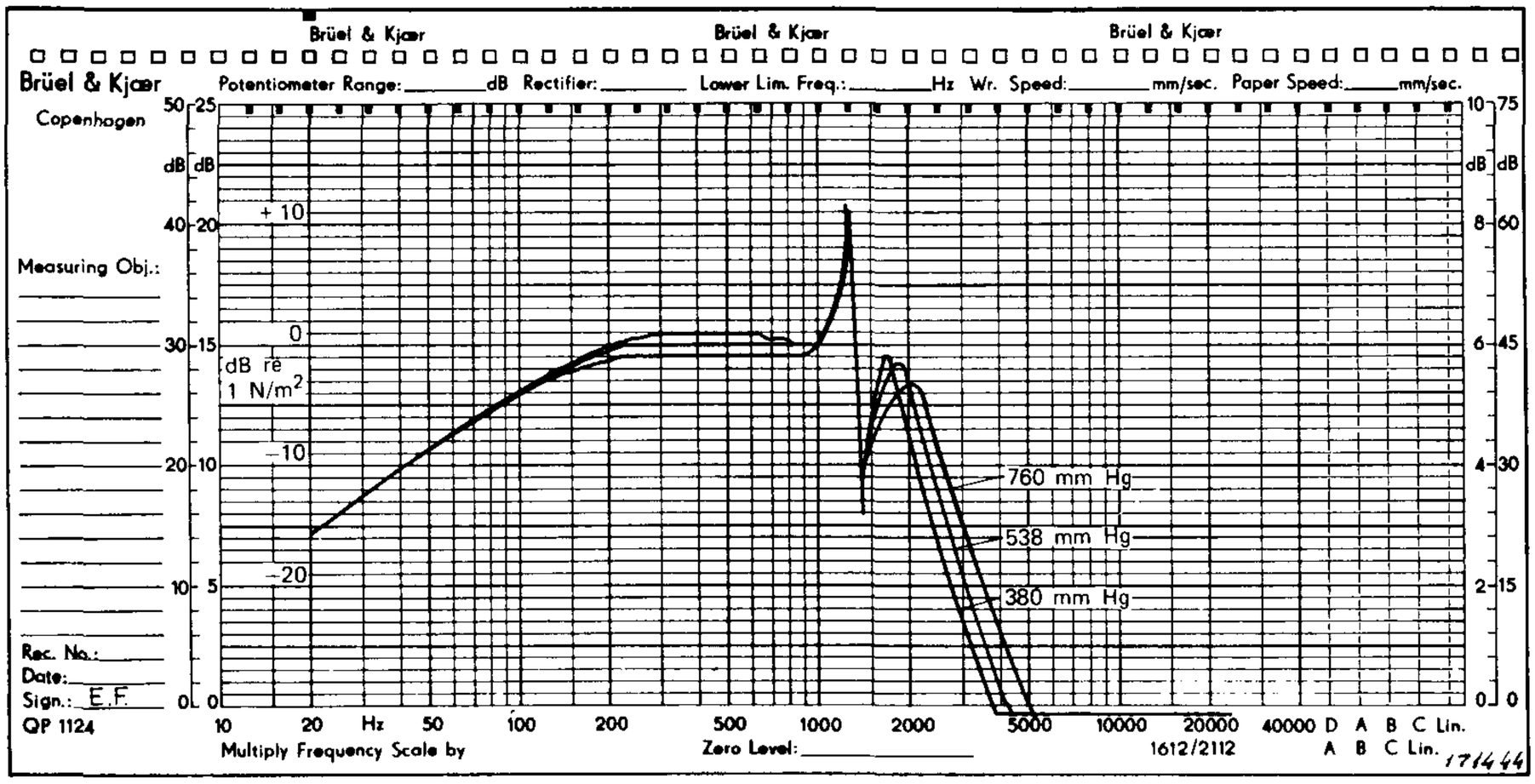

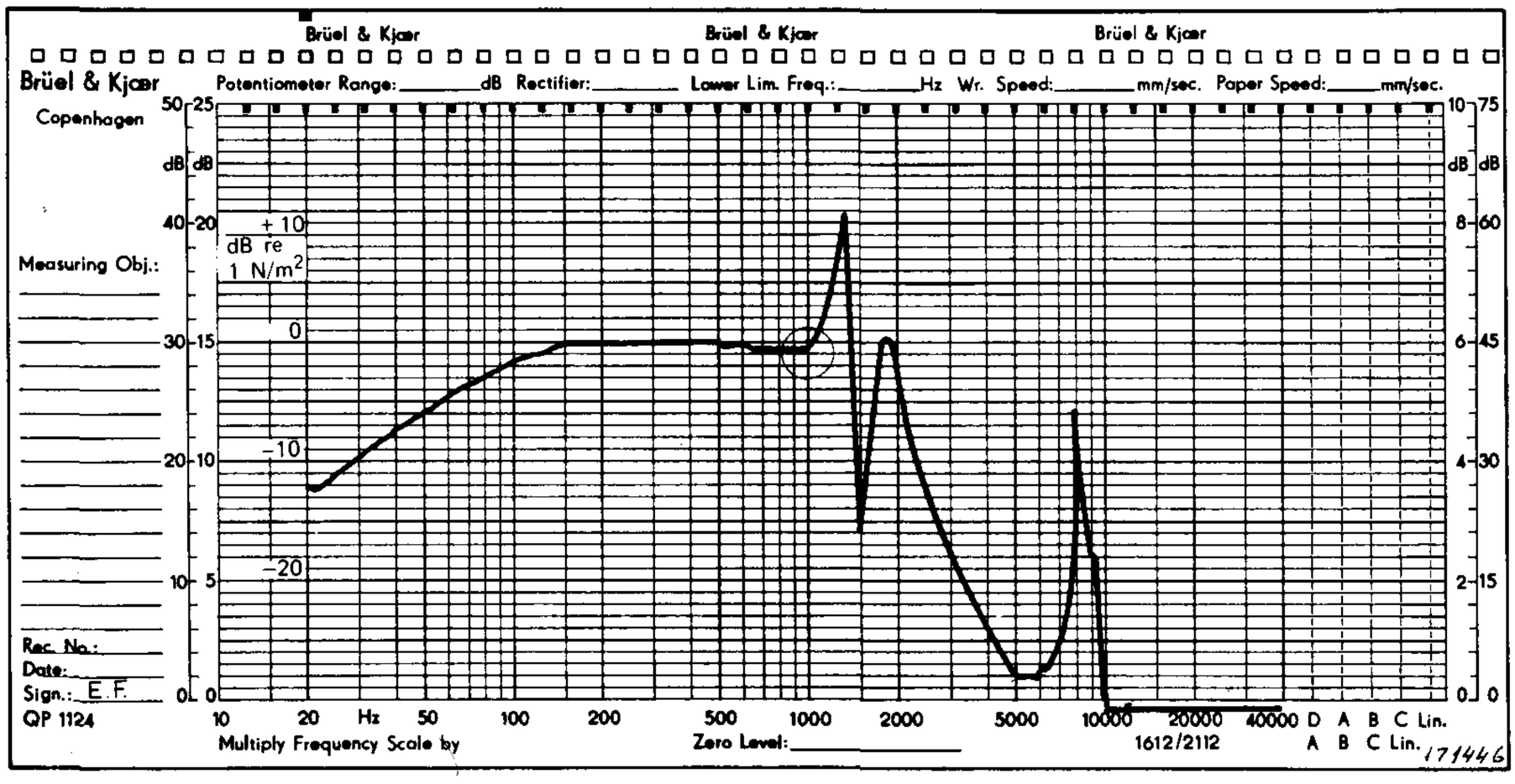

Fig.6. The sound pressure level measured as a function of frequency.
a. For the equivalent circuit
b. For the calibrator

The equivalent circuit has also been used for investigating the effects of individual elements on the stability of the calibrator. As regards stability, it can be said in general, that fewer the components, the more stable should the instrument be. The above described calibrator contains a number of elements, however, either they have practically no influence on the signal level at 1000 Hz, or they are expected to be very stable. Nevertheless, the calibrator in this respect cannot be compared to piston-type calibrators.

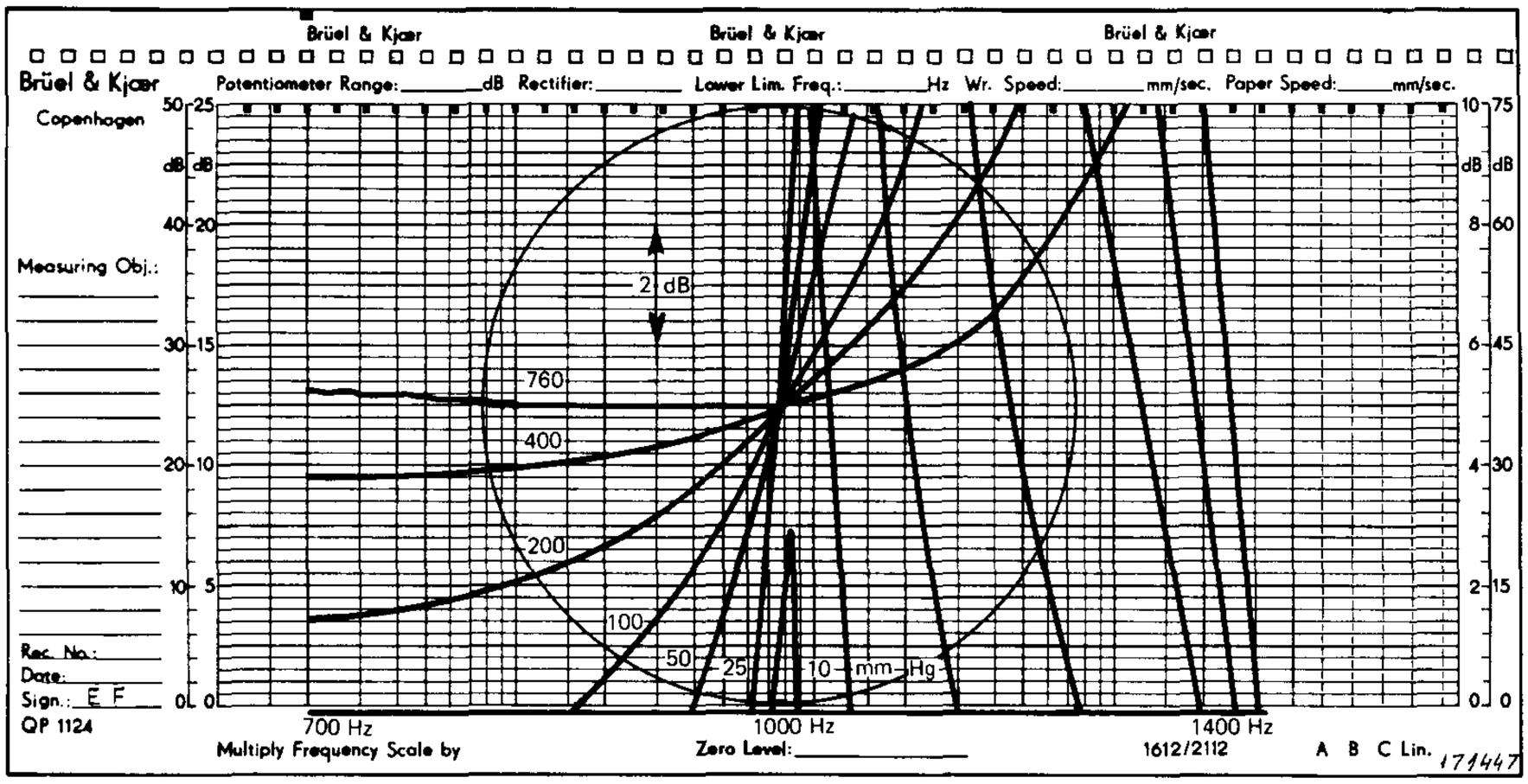

Fig.7. Sound pressure level measured against frequency for the calibrator at 1000 Hz for various atmospheric pressures. (The circle refers to the one on Fig.6b but to an enlarged scale)

The calibrator has not been developed with the aim for use in the laboratory, but rather for field measurements, rendering ease of use, and eliminating corrections for atmospheric pressure and equivalent volume.

News from the Factory

Heterodyne Voltmeter Type 2007

The new Heterodyne Voltmeter is a completely self-contained, precision instrument designed to measure directly voltages in AM-FM, single sideband, and television frequency ranges. It will determine the voltage level, the frequency, and the modulation percentage of an input signal. The instrument can be powered from AC main, built-in batteries (recharger included), or external batteries.

The Heterodyne Voltmeter Type 2007 is developed from Type 2006. Type 2007 is equipped with electronic control of the variable oscillator, and the frequency range is 100 kHz to 305 MHz in eight overlapping ranges. The tuned frequency is indicated on a moving coil meter provided with interchangeable scales. Three scales are included, a general frequency scale, a scale for American TV channels, and one for European TV channels. Scales can be custom made to order.

The Heterodyne Voltmeter Type 2007 has been designed with an untuned input and a mixer circuit with an ultra flat frequency response. With the normal type of instrument having a tunable input, recalibration is necessary at each frequency due to the corresponding "Q" changes. However, the B & K Type 2007 establishes self-calibration from a built-in stabilized 27 MHz reference oscillator. After calibration, further adjustments are not necessary while sweeping the entire frequency range from 100 kHz to 305 MHz.

The input probe contains a high impedance FET stage providing minimum load of the circuit being measured. A 50Ω probe extension is included for measurements on high frequency transmission lines. The normal voltage measuring range covers 100 μV to 100 mV full scale deflection. The built-in attenuator provides seven accurate 10 dB steps in sensitivity. A 60 dB attenuator is provided which, when fitted to the input probe, extends the range to 100 V.

In the six higher frequency ranges covering 7 to 305 MHz a triple-detection receiver is used providing double conversion. This design gives more than 50 dB image-frequency and intermediate frequency rejection also in these ranges.

A crystal filter following the mixer stage provides a "narrow" measurement bandwidth of ± 1.25 kHz. By switching out this filter a "wide" bandwidth

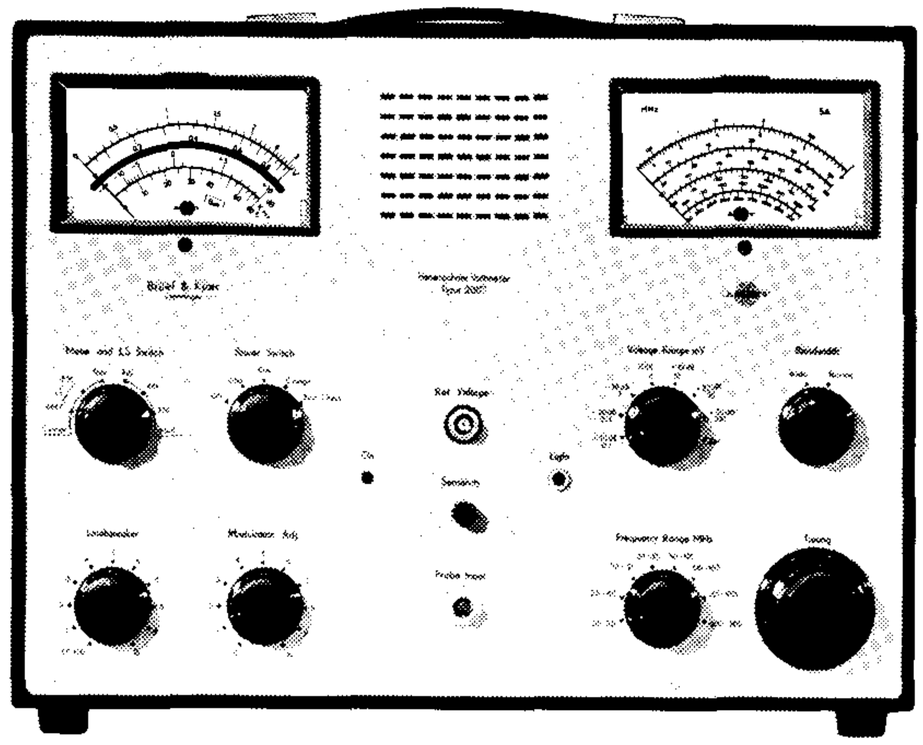

of ± 100 kHz is obtained. Option available for modification to fulfil the CISPR requirements.

The Heterodyne Voltmeter has a versatile readout system, featuring four major output indicators: a dual function meter for voltage level and modulation, the frequency indication meter, and a built-in loudspeaker for signal identification. A peak detector is built-in for TV measurements.

Heterodyne Analyzer Type 2010

The new Heterodyne Analyzer Type 2010 is designed as a multi-purpose high precision analyzer which finds its use in applications within various fields of research and routine measurements. It is ideally suited for work in acoustics, electroacoustics and vibration.

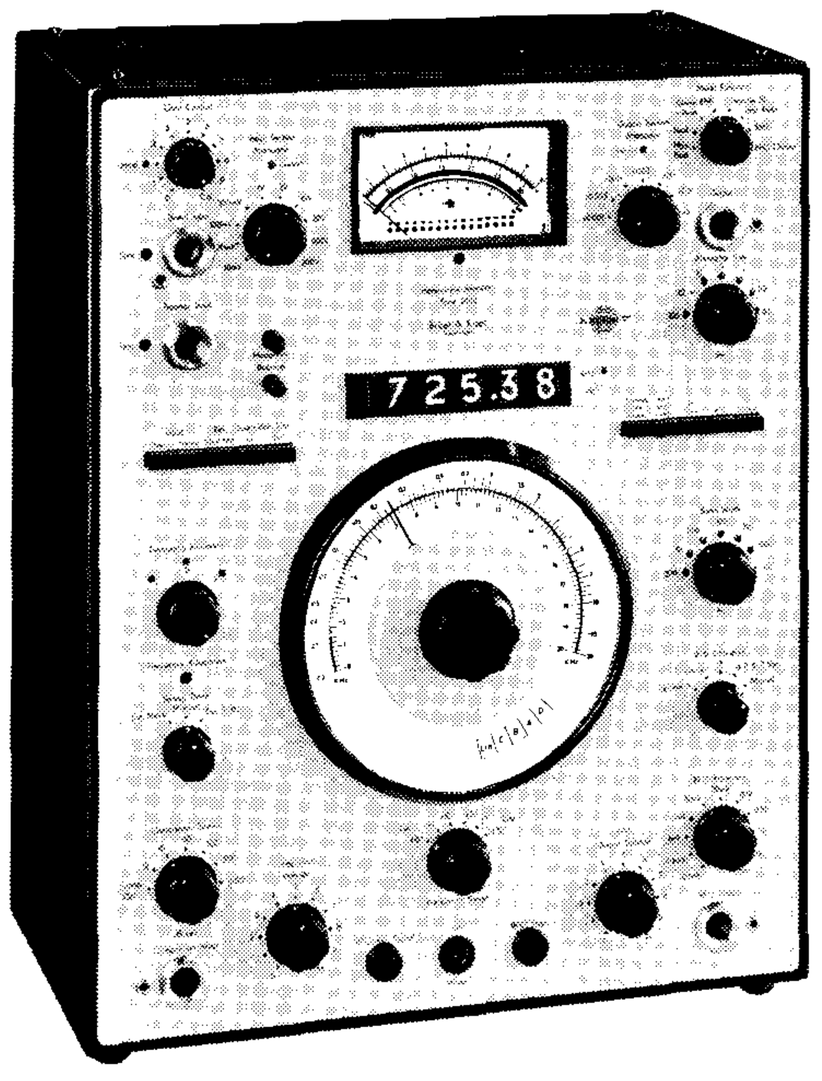

It is a constant bandwidth narrow band frequency analyzer covering the frequency range of 2 Hz to 200 kHz in three ranges. The three ranges 2 Hz to 2 kHz, 20 Hz to 20 kHz and 200 Hz to 200 kHz are continuously tuneable, and linear as well as logarithmic scanning can be selected. A, B, C and D weighting networks are built-in.

The measuring amplifier contained is similar to the Type 2607 but without impulse and peak indication. The meter indicates true RMS value for signals with crest factors up to 5 and the rectifier circuit has averaging times selectable in the range from 0.1 to 100 seconds. The meter has inter-changeable scales, automatic zero level indication and the standardized dampings Fast and Slow for sound level measurements. The meter circuit has AC as well as DC output for recorders and a lin-log converter allows for linear and logarithmic meter indication.

The filter section which contains double two pole Butterworth filters provides six selectable constant bandwidths (3.5 dB) in the range from 3.16 Hz to 1000 Hz and has a dynamic range greater than 85 dB.

For measurement of Power Spectral Density, the analyzer is equipped with a B and T program which allows Bandwidth and Averaging time to be varied automatically with frequency at 5 fixed cross-over frequencies thus main-taining the same confidence level over the entire frequency range. Three program modes are available: B variable, T variable or B and T variable (B x T constant). The B and T program can also be controlled externally.

Bandwidth compensation according to $1/\sqrt{B}$ is available. The analyzer has output and input sockets in order to facilitate the use of external filters and signals for synchronizing the Heterodyne Slave Filter Type 2020 are incorporated.

The frequency sweep of the analyzer can be controlled manually, mechanically from external drive or electrically by means of an external DC voltage. Facilities are provided for easy calibration of recording paper, by marker pulses.

A built-in automatic frequency control can be used for the 4 lower band-widths for resonance testing and the frequency is displayed on a six digit Nixie display for high accuracy.

The output voltage of the BFO is adjustable in 10 dB steps from 0.1 mV to 10 V and continuously within each 10 dB step. (Output impedance is 600 Ω). A 5 Ω – 0.7 W output continuously adjustable from 0 to 10 V is

also available. For automatic level control the BFO has a compressor input with selectable compressor speeds and a range of 50 dB.

Measuring Amplifier, Type 2608

The Measuring Amplifier is an inexpensive member of the new Measuring Amplifier family from Brüel & Kjær which was introduced by the previously shown Types 2606 and 2607.

Like these two versions, it contains separated wide band (2 Hz to 200 kHz) input and output amplifiers to facilitate the use of external filters for frequency analysis.

Used with a B & K Condenser Microphone the 2608 fulfils the requirements for Precision Sound Level Meters of the IEC Recommendation 179 and of the german DIN 45633, part 1.

The meter indicates the true RMS value for a wide range of signals and the recorder output provides an AC signal (10 V RMS for full meter deflection) for recording on Level Recorders or for feeding to other instruments.

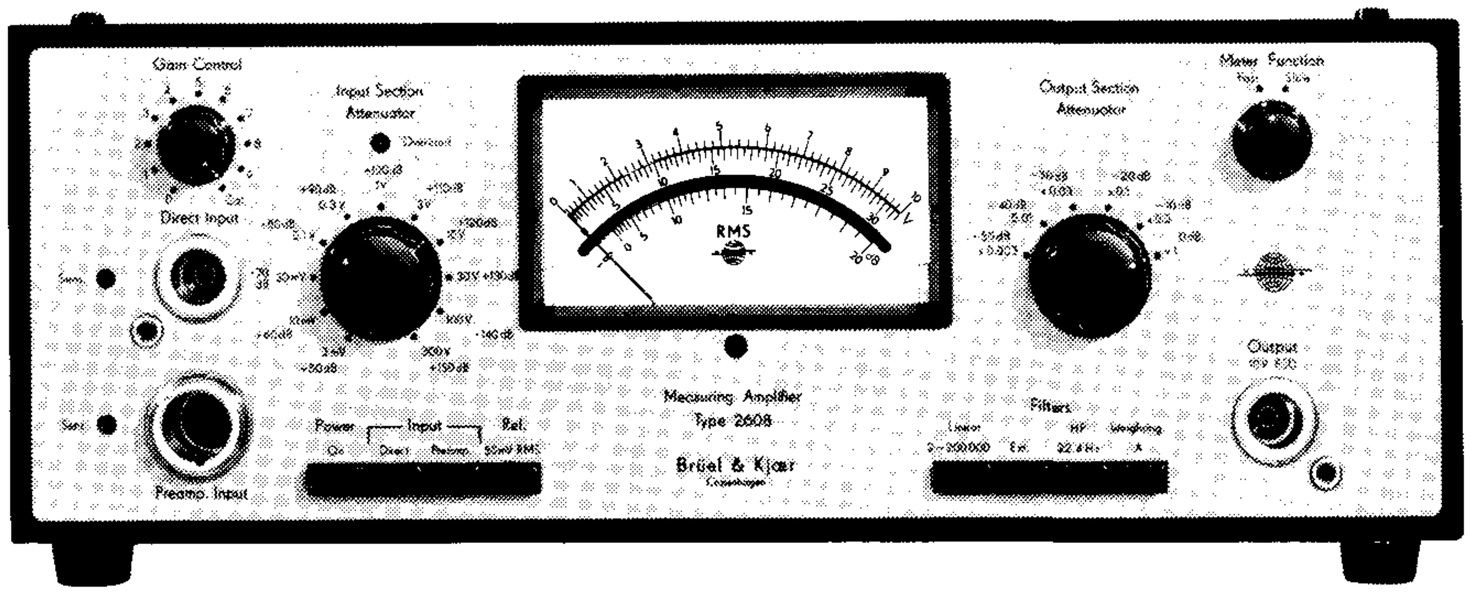

Insert Microphone Preamplifier Type 2627

Type 2627 is a Microphone Preamplifier intended for use with the B & K 1" Microphones Type 4144 and 4145. It's design facilitates insert voltage calibration of the microphones specified, in accordance with ANSI S 1.10 — 1966. A switch permits the 2627 to be used in either grounded shield or driven shield configurations.

A high impedance (10 GΩ) FET input stage ensures a low lower limiting frequency response, and a low broadband noise characteristic which gives a large dynamic range of the microphone/preamplifier combination.

The unit is powered from the microphone input of a B & K Measuring Amplifier or from the Microphone Power Supply Type 2803.

Tape Signal Gate, Type 2972

The Tape Signal Gate is a convenient means for gating the desired part of a signal to be transmitted to other instrumentation, as, for example, frequency analyzers and oscilloscopes. To trigger the gate, a reference signal (excitation signal or marking pulse) must precede the response signal to be analyzed by between 0.1 msec and 30 sec. The gate then transmits the analog signal for a time internal selectable between 0.1 msec and 30 sec.

Typical applications are in analysis of pulses using closed tape loops on tape recorders, where unwanted signals such as splice noise or switching transients can be eliminated (see Technical Review No. 3-1969, No. 3—1970 and No. 1-1971).

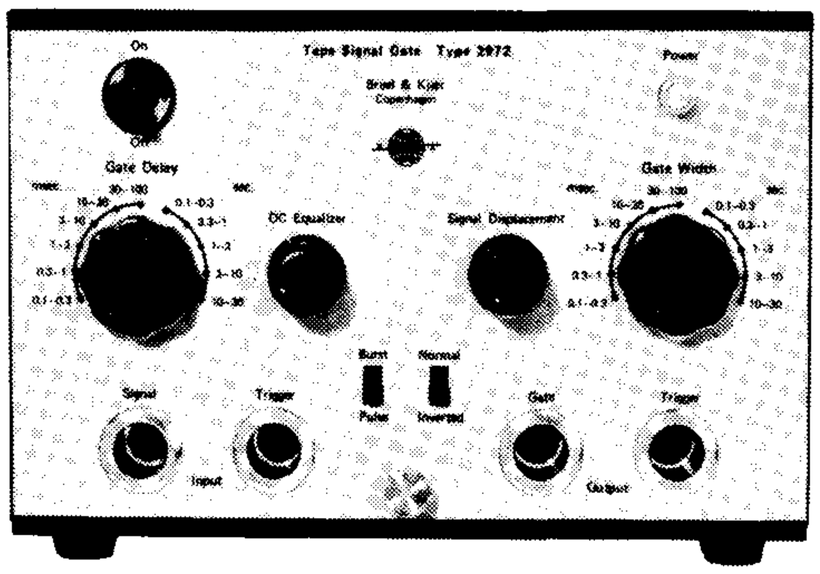

Artificial Voice Type 4219
The Artificial Voice Type 4219 has been designed for use in development and production control of small microphones and with particular regard for telephone transmitters where a well defined sound source is required. The sound field near the Voice in the region occupied by telephone transmitters, closely follows the distribution of the sound field from the human mouth.

The apparatus consists of a small loudspeaker mounted in a metal housing, a mouth piece a 1/4" regulating microphone mounted in the mouth opening and a built in microphone preamplifier. The microphone and preamplifier are supplied with the correct voltages when connected to any of the B & K Measuring Amplifiers, Frequency Analysers or Microphone Power supplies. When the loudspeaker is fed by a signal from Beat Frequency Oscillator Type 1022 and regulated automatically by the regulating microphone, the sound pressure level in front of the mouth piece can be kept constant to within ± 1 dB in the frequency range 50 Hz to 10 kHz. On account of the regulating feature the voice has an extremely low impedance making it useful for testing microphone mounted in closed masks and as a constant sound pressure source for testing silencers etc.

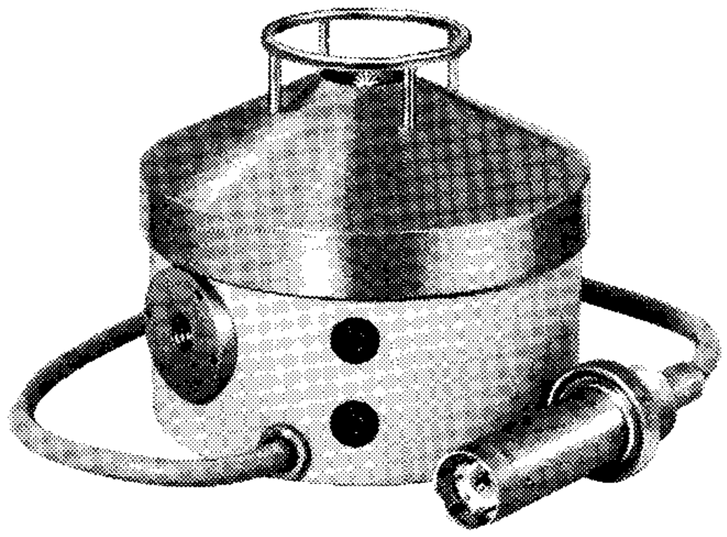

Accelerometer Calibrator and Preamplifier Type 4292
This instrument contains a small calibration exiter and a preamplifier with integrating networks. The unit is powered from a Measuring Amplifier or a Microphone Power Supply.

The calibrator is driven by an internal 79.6 Hz ($\omega = 500\ \text{sec}^{-1}$) generator and it is used to vibrate accelerometers of up to 70 grammes mass to an acceleration level of 1 g peak which is indicated by the rattle method. The rattling ball is enclosed in a replaceable hermetically sealed cylinder.

The whole calibrator section is spring suspended to isolate it from ambient vibration; and its moving system is adjusted to resonance for different loads

by a knob on the rear panel, which controls the tension and thereby the stiffness of the moving system spring.

Final adjustment of the vibration level is performed by a voltage control potentiometer on the front panel.

The preamplifier has adjustable gain from 0 to 20 dB. Together with the integrating networks this allows convenient measurement of acceleration, velocity and displacement for a wide range of signal frequencies.

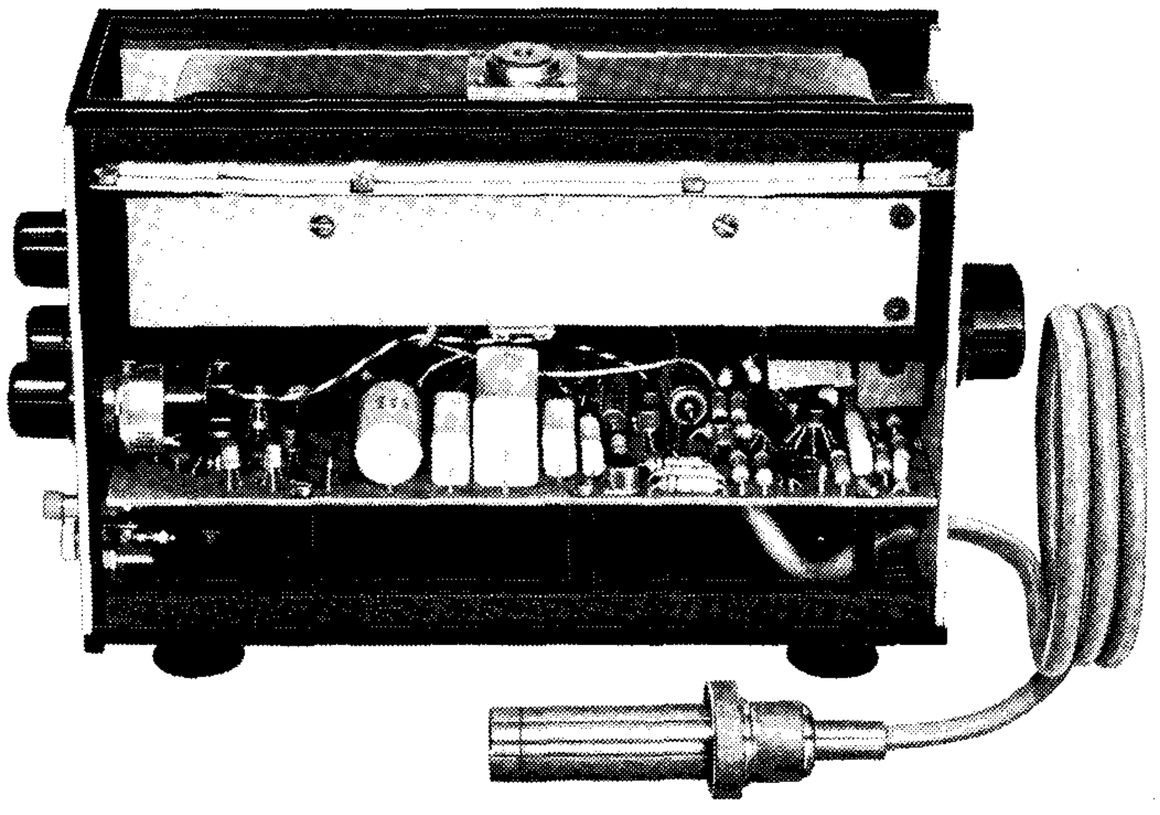

Vibration Exciter System M. 1200/1500 lb Force

Following the introduction of the 100 lbf and 400 lbf interchangeable head Vibration Exciter Systems "V" and "S" in April 1971 we now have pleasure in announcing the 1200/1500 lbf (5340/6670 N) System M.

System M consists of an Exciter Body, four easily interchangeable Exciter Heads, and a 6 kVA Power Amplifier, with type numbers as follows:

Exciter Body	Type 803
High g Head	Type 821
General Purpose Head	Type 822
Big Table Head	Type 823
Mode Study Head	Type 824
Power Amplifier	Type 709
Alternative Exciter Body with open frame base	Type 853
Alternative Power Amplifier with reduced power	Type 732

The M System retains the unique design features of the smaller "S" and "V" Systems, maintaining the same degree of versatility, precision and reliability together with the comprehensive metering and protective functions which

ensure that no part of the system is overdriven or damaged. We refer the reader to Galt Booth's paper entitled "Interchangeable Head Vibration Exciters" and to "News from the factory" in Technical Review No. 2-1971 where the B & K Vibration exciter programme is discussed in detail.

Alternative Exciter Body Type 853 has an open frame base with a single suspension system and facility for either vertical or horizontal working. The air cooling and field supply systems are remote and flexibly coupled to the exciter.

Alternative Power Amplifier Type 732 is a de-rated version of the 6 kVA type 709, having a power output of 3 kVA. When used with the Type 732, the maximum velocity limit for the M exciters is reduced from 50 in/s (1.7 m/s) to 25 in/s (0.635 m/s).

PREVIOUSLY ISSUED NUMBERS OF BRÜEL & KJÆR TECHNICAL REVIEW

(Continued from cover page 2)

3–1968 On the Measurement and Interpretation of Cross-Power-Spectra.
Cross Power Spectral Density Measurements with Brüel & Kjær Instruments (Part 1).
2–1968 The Anechoic Chambers at the Technical University of Denmark.
1–1968 Peak Distribution Effects in Random Load Fatigue.
4–1967 Changing the Noise Spectrum of Pulse Jet Engines.
On the Averaging Time of Level Recorders.
3–1967 Vibration Testing – The Reasons and the Means.
2–1967 Mechanical Failure Forecast by Vibration Analysis.
Tapping Machines for Measuring Impact Sound Transmission.
1–1967 FM Tape Recording.
Vibration Measurements at the Technical University of Denmark.
4–1966 Measurement of Reverberation.
3–1966 Measurement and Description of Shock.
2–1966 Some Experimental Tests with Sweep Random Vibration.
1–1966 Windscreening of Outdoor Microphones.
A New Artificial Mouth.

SPECIAL TECHNICAL LITERATURE

As shown on the back cover page Brüel & Kjær publish a variety of technical literature which can be obtained free of charge. The following literature is presently available:

Mechanical Vibration and Shock Measurements (English, German)
Acoustic Noise Measurements (English), 2. edition
Architectural Acoustics (English)
Power Spectral Density Measurements and Frequency Analysis (English)
Standards, formulae and charts (English)
Lectures and exercises for educational purposes
Instruction manuals (English, German, French, Russian)
Catalogs (several languages)
Product Data Sheets (English, German, French, Russian)

Furthermore, back copies of the Technical Review can be supplied as shown in the list above. Older issues may be obtained provided they are still in stock.

BRÜEL & KJÆR

DK-2850 Nærum, Denmark. Teleph.: (01) 80 05 00. Cable: BRUKJA, Copenhagen. Telex: 15316